AD-A187 083 MULTIDIMENSIONAL SYSTEM ANALYSIS OF ELECTRO-OPTIC SENSORS WITH SAMPLED DETERMINISTIC OUTPUT(U) NAVAL RESEARCH LAB WASHINGTON DC M S LONGMIRE ET AL 1/1

UNCLASSIFIED 18 DEC 87 NRL-MR-6106 F/G 17/5 NL

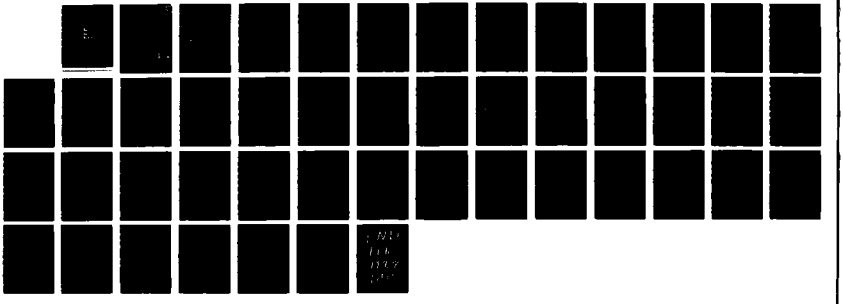

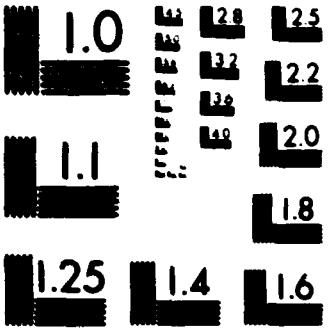

Naval Research Laboratory
Washington, DC 20375-5000



NRL Memorandum Report 6106



# Multidimensional System Analysis of Electro-optic Sensors with Sampled Deterministic Output

M. S. LONGMIRE

*Department of Physics and Astronomy*
*Western Kentucky University*
*Bowling Green, KY 42101*

D. A. SCRIBNER

*Electro-optical Technology Branch*
*Optical Sciences Division*

December 18, 1987

SECURITY CLASSIFICATION OF THIS PAGE

## REPORT DOCUMENTATION PAGE

Form Approved OMB No 0704-0188

AD-A187083

| | |
|---|---|
| 1a. REPORT SECURITY CLASSIFICATION<br>UNCLASSIFIED | 1b. RESTRICTIVE MARKINGS |
| 2a. SECURITY CLASSIFICATION AUTHORITY | 3. DISTRIBUTION / AVAILABILITY OF REPORT<br>Approved for public release; distribution unlimited. |
| 2b. DECLASSIFICATION / DOWNGRADING SCHEDULE | |
| 4. PERFORMING ORGANIZATION REPORT NUMBER(S)<br>NRL Memorandum Report 6106 | 5. MONITORING ORGANIZATION REPORT NUMBER(S) |
| 6a. NAME OF PERFORMING ORGANIZATION<br>Naval Research Laboratory<br>6b. OFFICE SYMBOL (If applicable)<br>Code 6550 | 7a. NAME OF MONITORING ORGANIZATION |
| 6c. ADDRESS (City, State, and ZIP Code)<br>Washington, DC 20375-5000 | 7b. ADDRESS (City, State, and ZIP Code) |
| 8a. NAME OF FUNDING / SPONSORING ORGANIZATION<br>Naval Surface Weapons Center<br>8b. OFFICE SYMBOL (If applicable) | 9. PROCUREMENT INSTRUMENT IDENTIFICATION NUMBER |
| 8c. ADDRESS (City, State, and ZIP Code)<br>White Oak, Silver Spring, MD 20903-5000 | 10. SOURCE OF FUNDING NUMBERS<br>PROGRAM ELEMENT NO: 62111N; PROJECT NO.; TASK NO; WORK UNIT ACCESSION NO: 65-2465-0-7 |

11. TITLE (Include Security Classification)
Multidimensional System Analysis of Electro-optic Sensors with Sampled Deterministic Output

12. PERSONAL AUTHOR(S)
Longmire, M. S.* and Scribner, D. A.

| 13a. TYPE OF REPORT | 13b. TIME COVERED | 14. DATE OF REPORT (Year, Month, Day) | 15. PAGE COUNT |
|---|---|---|---|
| Interim | FROM _____ TO _____ | 1987 December 18 | 47 |

16. SUPPLEMENTARY NOTATION
*Western Kentucky University, Bowling Green, KY 42101

| 17. COSATI CODES | | | 18. SUBJECT TERMS (Continue on reverse if necessary and identify by block number) |
|---|---|---|---|
| FIELD | GROUP | SUB-GROUP | Electro-optic system analyses, Staring sensors, Temporal sampling, Scanning sensors, Spatial sampling |
| | | | |
| | | | |

19. ABSTRACT (Continue on reverse if necessary and identify by block number)

System descriptions of scanning and staring electro-optic sensors with sampled output are developed as follows. Functions representing image formation, detector response, and analog processing of detector output are formulated in the space and time domain. Then the types of sampling permitted by sensor motion, spatial integration of image irradiance, and temporal integration of sensor output are discussed. Next functions representing sensor output sampled in each of these ways are constructed. The relations for a staring sensor describe a temporal sequence of images; those for a scanning sensor represent a single sampled image. Finally, the space and time domain functions are fourier transformed to the spatial- and temporal-frequency domain to complete the system descriptions. The results should be useful for designing electro-optic sensor systems and correcting data for instrumental effects and other experimental conditions.

| | |
|---|---|
| 20. DISTRIBUTION / AVAILABILITY OF ABSTRACT<br>☒ UNCLASSIFIED/UNLIMITED ☐ SAME AS RPT ☐ DTIC USERS | 21. ABSTRACT SECURITY CLASSIFICATION<br>UNCLASSIFIED |
| 22a. NAME OF RESPONSIBLE INDIVIDUAL<br>D. A. Scribner | 22b. TELEPHONE (Include Area Code)<br>202-767-2225<br>22c. OFFICE SYMBOL<br>Code 6552 |

DD Form 1473, JUN 86 Previous editions are obsolete SECURITY CLASSIFICATION OF THIS PAGE

S/N 0102-LF-014-6603

## CONTENTS

## LIST OF SYMBOLS

### Nonalphabetic Characters

' (apostrophe or prime)....Designates the image plane, its absence the object (background) plane, Fig. 1; used with both coordinates and physical quantities, e.g., $[(x',y'),(x,y)]$ and $[u'_\lambda,u_\lambda]$.

$\equiv$ (identity).....Signifies a definition.

; (semicolon).....Separates variables from parameters in an argument list - (variables;parameters).

$\rightarrow$ (arrow).....Marks chief space- and time-domain equations.

$\cdot$ (midline dot).....Placed between factors of a product to facilitate recognition.

$\circledcirc$ (copyright sign).....Signifies convolution of two functions with respect to one variable, i.e., $g(x)\circledcirc w(x^\circ-x) \equiv \int_{-\infty}^{\infty} g(x)\cdot w(x^\circ-x)\cdot dx = z(x^\circ)$; repetition indicates multiple convolution.

° (degree).....Marks the variable or parameter of a convolution integral; may be affixed to either.

` (grave accent).....Denotes sampling by a comb function.

\ \ (backslashes).....Signify cropping of an image in space and truncation of an image sequence in time.

< > (angular brackets).....Indicate linear, shift-invariant, temporal averaging of sensor output during temporal-integral sampling.

$\Leftrightarrow$ (double arrow).....Identifies a fourier transform pair.

$\hat{}$ (circumflex or hat).....Marks vectors.

$\tilde{}$ (tilde).....Affixed to one member of a fourier pair to indicate distortion ("rippling") due to truncation of the other member.

### Subscripts

a.....An atmospheric quantity.

b.....A background (object) quantity.

c.....Labels central coordinates of detector elements and integration intervals.

f.....“Filtered”, i.e., passed through one or more stages of linear, shift-invariant, analog processing.

g.....A gaussian (ideal geometric-optical) quantity.

$\lambda$.....A spectral quantity, one resulting from radiation in the infinitesimal wavelength range $\lambda$ to $(\lambda+d\lambda)$; also a monochromatic quantity, the value of a wavelength-dependent quantity at wavelength $\lambda$.

## Latin Letters

a.....Detector width (x dimension), Figs. 2 and 3.
A.....Area of optical aperture stop, Fig. 1.
b.....Detector height (y dimension), Figs. 2 and 3.
d.....Distance from optical aperture to object, Fig. 1; also indicates an infinitesimal quantity, e.g., $d\lambda$.
D.....Diameter of a circular aperture stop.
f.....Temporal frequency.
$\Delta f$.....Temporal frequency interval ($\Delta f = 1/\Delta t$).
$\Delta F$.....Temporal frequency interval ($\Delta F = 1/\Delta T$).
$F_L$.....Equivalent focal length of optics, Fig. 1; $F_L = -(x'_g/x_b)d = -(y'_g/y_b)d$.
$F^{\#}_{eff}$.....Equivalent "F" number of optics with a circular aperture stop; $F^{\#}_{eff} = F_L/D$.
${}^3F[\ ]$, ${}^2F[\ ]$, ${}^1F[\ ]$.....Three-, two-, and one-dimensional fourier transformation, Eq. (30) et seq..
${}^{-3}F[\ ]$,${}^{-2}F[\ ]$,${}^{-1}F[\ ]$.....Inverse three-, two-, and one-dimensional fourier transformation, Eq. (31) et seq..
$g \Leftrightarrow G$.....An arbitrary space-time function and its fourier transform (spectrum).
$h(t) \Leftrightarrow H(f)$.....Overall impulse response and transfer function for all stages of linear, shift-invariant, analog processing of detector output including, if applicable, temporal averaging during temporal-integral sampling.
i.....Imaginary unit, $i^2 = -1$.
$k_x, k_y$.....Magnitudes of components of spatial frequency vectors $\hat{k} = \hat{k}_x + \hat{k}_y$.
$\Delta k_x, \Delta k_y$.....Intervals of $k_x$ and $k_y$.
l,m,n.....Integers labeling spatial (l,m) and temporal (n) sample sites; also summation indices of sampling functions, Eqs. (23a,b). Spatial coordinates of sample sites are $(l\Delta x, m\Delta y)$, Fig. 3.
L,M.....Number of rows (M) and columns (L) of samples

in cropped images. (L-1),(M-1) are maximum values of summation indices (l,m) in functions representing sampled and cropped images. Fig. 4, Eqs. (28a,b) and (29a,b).

$n_{b\lambda} \Leftrightarrow N_{b\lambda}$.....Background near-normal spectral radiance, Fig. 1, and its fourier transform.

$p_\lambda \Leftrightarrow P_\lambda$.....$p_\lambda$ is the monochromatic point-spread function. $P_\lambda$ is the monochromatic optical transfer function. Both are for a geometric-optical projection of the image onto the object plane and are expressed in object-plane quantities.

$p'_\lambda$.....Monochromatic point-spread function in the image plane. $p'_\lambda$ is expressed in image-plane quantities; $p'_\lambda = p_\lambda/\mu^2$.

$q \Leftrightarrow Q$.....An arbitrary space-time function and its fourier spectrum.

rcm and rmr.....Reciprocal centimeter and reciprocal milliradian, units of spatial frequency.

$R_\lambda$.....Peak value of monochromatic responsivity on the surface of a detector element.

S.....Surface of a detector element, Fig. 2.

s.....Detector or sensor output before measurement. The unit may be [amps, carriers/sec, volts, etc.] depending on the corresponding unit of $R_\lambda$.

$s_\lambda \Leftrightarrow S_\lambda$.....Spectral output of a detector element and fourier transform of $s_\lambda$, Eqs. (19a,b) and (43a,b).

$s_{\lambda f} \Leftrightarrow S_{\lambda f}$.....The pseudoimage and its fourier spectrum. $s_{\lambda f}$ is analog-processed spectral output of a detector element whose center may be located anywhere in space. Eqs. (20a,b), (21a,b), (46a,b), and (47a,b).

$\langle s_{\lambda f} \rangle$.....The pseudoimage when analog processing includes temporal averaging of $s_\lambda$ during temporal-integral sampling.

t.....Time.

$\Delta t$.....Intraimage sampling period (time between samples) for an image from a scanning sensor; $\Delta t = \Delta x/\zeta$, Fig. 3.

T.....The epoch of an image (data frame), i.e., time at a chosen moment during image acquisition.

$\Delta T$ ..... Time between images, i.e., interimage (interframe) sampling period.

$u_{b\lambda} \Leftrightarrow U_{b\lambda}$ ..... Apparent background spectral irradiance and its fourier transform, Eqs. (2a,b) and (39a,b). Both include atmospheric properties $\theta_{a\lambda}$ and optical parameters $[\theta_\lambda \cdot (A/d^2]$.

$u'_{g\lambda}$ ..... Spectral irradiance distribution in a gaussian image, Eq. (4).

$u'_\lambda$ ..... Spectral irradiance distribution in the actual image. Fig. 1, Eqs. (8) and (11).

$u_\lambda \Leftrightarrow U_\lambda$ ..... $u_\lambda$ is the spectral irradiance distribution in the image after geometric-optical projection onto the object plane, Fig. 1. $U_\lambda$ is the fourier transform of $u_\lambda$, Eqs. (13a,b) and (40a,b).

$v$ ..... Detector or sensor output after measurement. The unit is assumed to be volts, requiring the corresponding unit of $R_\lambda$ to be volts.

$\dot{v}_{\lambda f} \Leftrightarrow V_{\lambda f}$ ..... An instantaneously sampled pseudoimage $s_{\lambda f}$ and its fourier transform, Eqs. (24a,b) and (49a,b).

$\backslash \dot{v}_{\lambda f} \backslash \Leftrightarrow \tilde{V}_{\lambda f}$ ..... An instantaneously sampled and cropped pseudoimage $s_{\lambda f}$ and its fourier transform, Eqs. (28a,b) and (50a,b).

$\langle \dot{v}_{\lambda f} \rangle, \backslash \langle \dot{v}_{\lambda f} \rangle \backslash$ ..... These represent $\dot{v}_{\lambda f}$ and $\backslash \dot{v}_{\lambda f} \backslash$ when formation of the pseudoimage $s_{\lambda f}$ includes temporal averaging during temporal-integral sampling. Eqs. (26a,b),(29a,b).

$w \Leftrightarrow W$ ..... An arbitrary space-time function and its fourier spectrum.

$(x,y),(x',y')$ ..... Object- and image-plane coordinates, Fig. 1.

$(x_b,y_b),(x'_g,y'_g)$ ..... Coordinates of a background (object) point and its ideal geometric-optical image point, Fig. 1.

$(\Delta x',\Delta y')$ ..... Image-plane coordinates $(x'-x'_g,y'-y'_g)$ measured from a gaussian image point, Fig. 1.

$(x_c,y_c)$ ..... Central coordinates of a detector element after geometric optical projection onto the object plane, Figs. 2 and 1.

$\Delta x,\Delta y$ ..... Spatial sampling intervals, Figs. 3 and 4.

$z \Leftrightarrow Z$ ..... An arbitrary space-time function and its fourier spectrum.

## Greek Letters

$(\alpha,\beta)$.....Detector-center coordinates for analog processing of detector output $s_\lambda$, i.e., pseudo-image ($s_{\lambda f}$) coordinates corresponding to $(x_c,y_c)$, Eqs. (20a,b) and (21a,b); also central coordinates of all possible areas for integration of image irradiance by the detector, Fig. 3.

$\gamma \Leftrightarrow \Gamma$.....Detector-response function and detector transfer function. $\gamma$ describes the photosensitive surface of a detector element (Fig. 2) and any variation of responsivity on that surface.

$\varepsilon$.....Sampling duration, i.e., time required to measure a sample.

$\zeta$.....Scan rate.

$\theta_{a\lambda},\theta_\lambda$.....Monochromatic transmittances of atmosphere and optics.

$\lambda$.....Radiant wavelength.

$\mu$.....Optical magnification = $x'_g/x_b = y'_g/y_b$, Fig. 1.

$\tau$.....Time at which output from analog processing occurs, Eqs. (20a,b) and (21a,b).

$\Psi_\lambda,\Psi'_\lambda$.....Incoherent, spectral, radiant flux at object and image planes, Eqs. (1),(6),(7).

# MULTIDIMENSIONAL SYSTEM ANALYSIS OF ELECTRO-OPTIC SENSORS WITH SAMPLED DETERMINISTIC OUTPUT

## I. INTRODUCTION

Much effort has been and is being devoted to collection of optical background data. The utility of these data would be increased significantly if it were possible to calculate from them the values that would have been measured in the same circumstances with an optical sensor of lower spatial resolution and sampling rate. There have been intuitively based attempts to do this, but to know whether or to what extent the results are valid, the computations must be based on a more rigorous and comprehensive analysis of the sensor and sampling.

Such an analysis is presented here. Staring sensors and one type of scanning sensor are treated; the scanner is the type that sweeps the image to and fro over the detector. System equations are derived initially in the space and time domain where the mathematics are easily related to physical reality. These equations then are fourier-transformed to the frequency domain to complete the system description. None of the material is wholly new. This is a review article whose purpose is to collect known results from diverse sources and provide them in a useful form in one place. The results can be used not only for synthesis of background data as mentioned, but also for equalization (correction of data for instrumental effects), and for engineering of electro-optic sensor systems.

## II. SPACE- AND TIME-DOMAIN DERIVATIONS

With one exception the treatment will follow physical and experimental order, according to which the equations fall into groups describing image formation, detector response, analog processing, sampling of sensor output, and image cropping. Cropping or truncation of the image is formulated last for mathematical convenience, although physically it occurs during image formation or sampling. Functions representing the analog outputs of the sensors are constructed first. Next the types of sampling permitted by sensor motion, spatial integration of image irradiance, and temporal integration of sensor output are described. Lastly functions representing sensor output sampled in each of these ways are formulated. The relations for staring sensors depend on time and two spatial coordinates, and the results describe a temporal sequence of sampled images. Scanning links time and the spatial coordinate in the scan direction. Consequently, the relations for scanning

Manuscript approved October 2, 1987.

sensors are only two dimensional; they depend either on two spatial coordinates or on time and the cross-scan spatial coordinate. Moreover, the results describe only one sampled image. This restriction stems from the functions used to represent the space-time constraint and the sampling.

The functions that describe the optics vary only with the spatial coordinates; those that describe analog processing vary only with time; and those that describe sampling vary with both the spatial and the temporal coordinates. Thus a coordinate can be a variable or a parameter at different stages of the analysis. The two types of dependence are distinguished by placing variables on the left of a semicolon separating the arguments of a function, e.g., $w(x,y,t)$, $w(x,y;t)$, $w(t;x,y)$. All independent coordinates can be separately varied or held constant at any stage of the analysis. But if a spatial or temporal coordinate that has been a parameter is subsequently varied, or vice versa, extra manipulations are required to derive the corresponding frequency-domain relations. A simpler alternative is always to keep the full complement of variables in the space-time equations. This can be done by convolving the equations with delta functions. The technique is further explained when used. It can always be assigned physical meaning.

All derivations are given in detail. This has advantages and drawbacks. The chief advantages are that assumptions and approximations are made evident, and the results can be used or modified easily for computations in a variety of circumstances. On the debit side, the details may hide the main results and the outline of the derivations. To combat this tendency, equations expressing the main results are marked with arrow prefixes $\Rightarrow$, and the analog output equations are summarized in subsection II.D using a concise notation. Anyone who wants an overview of the derivations can profitably refer to this subsection at any time. Because units are required for numerical work, typical units are given for most quantities, but other units can be used without changing the equations.

## A. Image Irradiance

Figure 1 represents an optical sensor viewing a distant source of incoherent radiation. The optics may have one element or several. The figure exhibits the coordinates and some of the notation as follows: A prime designates the image plane, its lack the object or background plane; a subscript b denotes a background quantity, its absence an image quantity. This seemingly redundant notation is employed for expository purposes. The letters n and u stand for radiance and irradiance; spectral and monochromatic quantities are indicated by a subscript $\lambda$ for wavelength. The distance from the optical aperture to the background is d; $F_L$ is the equivalent focal length. The aperture stop of area A

may or may not be circular; the field stop is a photosensitive detector in the image plane. Other notation will be introduced and defined as needed.

The object is viewed in a small field at near-normal incidence, allowing the sensor's subtense to be equated to $(A/d^2)$, and the directional dependence of object radiance to be neglected. The object's near-normal spectral radiance is $n_{b\lambda}(x_b,y_b)$ [watts/(cm$^2$·steradian·micron)], with temporal dependence momentarily disregarded. The combined transmittances of atmosphere and optics along a line of sight are $\theta_{a\lambda}\theta_\lambda$. Under these conditions the flux in wavelength range $\lambda$ to $(\lambda+d\lambda)$ collected by the optics from an area $(dx_b dy_b)$ at object point $(x_b,y_b)$ and imaged in the focal plane is (ref. 1, §5.5; ref. 2, §5.6; ref. 3, §11-5)

$$d^3\Psi_\lambda = \theta_{a\lambda}\theta_\lambda \cdot \left[n_{b\lambda} \cdot (dx_b dy_b) \cdot (A/d^2) \cdot d\lambda\right] \quad \text{[watts]}. \tag{1}$$

In order for detector output to be time dependent, $n_{b\lambda}$ in Eq. (1) must depend implicitly or explicitly on time. Scanning converts spatial dependence of radiance to temporal dependence. For treatment of scanning sensors, therefore, object radiance can be assumed time-independent during a scan and denoted by $n_{b\lambda}(x_b,y_b;T)$, with T specifying the epoch of the scan or image. With a staring sensor, object radiance must be an explicit function of time $n_{b\lambda}(x_b,y_b,t)$.

It is convenient to define an apparent background irradiance $u_{b\lambda}$, even though it has no physical significance.

$$\rightarrow u_{b\lambda}(x_b,y_b;T) \text{ or } u_{b\lambda}(x_b,y_b,t) \equiv \left(\frac{d^3\Psi_\lambda}{dx_b dy_b d\lambda}\right) \quad \text{[watts/(cm}^2\text{·micron)]}$$

$$\equiv \theta_{a\lambda} \cdot \left[\theta_\lambda (A/d^2)\right] \cdot \left[n_{b\lambda}(x_b,y_b;T) \text{ or } n_{b\lambda}(x_b,y_b,t)\right]. \tag{2a,b}$$

This simplifies notation and allows subsequent equations to be written more concisely. The physically significant quantities, however, are the optical parameters $[\theta_\lambda(A/d^2)]$, the atmospheric properties $\theta_{a\lambda}$, and the background radiance $n_{b\lambda}$. Further conciseness is achieved by omitting the spatial and/or temporal dependence of radiance and irradiance when no confusion is likely.

The points $(x_b,y_b)$ and $(x'_g,y'_g)$ in Fig. 1 are related through the optical magnification $\mu$, a negative number that accounts for image inversion and change of scale between the object and image planes. If image distortion (curvature) is negligible,

$$\mu = x'_g/x_b = y'_g/y_b = -F_L/d. \tag{3}$$

These equalities follow from the ray geometry of an optical system with a single converging thin lens, and they define the equivalent focal length of a compound optical system. If the aperture stop is circular, $A = \pi D^2/4$, and the equivalent "F" number is $F^{\#}_{eff} = F_L/D$. From these relations the subtense of the optics at the background is $(A/d^2) = (\pi/4)(\mu/F^{\#}_{eff})^2$. This equality can be used to replace the subtense in Eq. (2), but the apparent background irradiance still depends on background range through $\mu$ and $\theta_{a\lambda}$.

If the optics formed a gaussian (ideal geometric) image, $d^3\Psi_\lambda$ would illuminate an image area $(dx'_g dy'_g) = \mu^2(dx_b dy_b)$. The spectral irradiance of the geometric image then would be

$$u'_{g\lambda}(x'_g,y'_g) = \left(\frac{d^3\Psi_\lambda}{dx'_g dy'_g d\lambda}\right) = \frac{u_{b\lambda}(x_b,y_b)}{\mu^2} \quad [\text{watts}/(\text{cm}^2\cdot\text{micron})]. \tag{4}$$

In fact, flux from an object point is distributed in the image plane as described by the monochromatic point-spread function

$$p'_\lambda(x'_g,y'_g:x',y') = p'_\lambda(\mu x_b,\mu y_b:x',y') \quad [\text{cm}^{-2}]. \tag{5}$$

The point-spread function accounts for blurring of the image by diffraction and aberrations; other sources of blurring are mentioned later. The fraction of $d^3\Psi_\lambda$ that illuminates an image area $(dx'dy')$ is $p'_\lambda \cdot dx'dy'$. From this it is evident that $p'_\lambda$ has units of reciprocal area in the image plane and is normalized so that $\iint_{-\infty}^{\infty} p'_\lambda \cdot dx'dy' = 1$. The spectral flux received by $(dx'dy')$ from $(dx_b dy_b)$ is, therefore,

$$d^5\Psi'_\lambda = d^3\Psi_\lambda \cdot (p'_\lambda \cdot dx'dy') = (u_{b\lambda}\cdot dx_b dy_b d\lambda)(p'_\lambda \cdot dx'dy') \quad [\text{watts}]. \tag{6}$$

Now if $(x_b,y_b)$ is moved over the background, $(x'_g,y'_g)$ moves over the image, and flux increments from all object points can be summed to give the total flux at $(x',y')$:

$$d^3\Psi'_\lambda = \left[\iint_{-\infty}^{\infty} u_{b\lambda}(x_b,y_b)\cdot p'_\lambda(\mu x_b,\mu y_b:x',y')\cdot dx_b dy_b\right]\cdot dx'dy'd\lambda \quad [\text{watts}]. \tag{7}$$

The bracketed term in Eq. (7) is the actual image spectral irradiance,

$$u'_\lambda(x',y') = \left(\frac{d^3\Psi'_\lambda}{dx'dy'd\lambda}\right) = \iint_{-\infty}^{\infty} u_{b\lambda}\cdot p'_\lambda \cdot dx_b dy_b \quad [\text{watts}/(\text{cm}^2\cdot\text{micron})]. \tag{8}$$

Comparison of Eq. (8) with the geometric image irradiance Eq. (4) shows that the actual irradiance contains the scale factor $(1/\mu^2)$ implicitly in the point-spread function.

Eq. (8) expresses the image irradiance as a weighted linear superposition of the apparent background irradiance $u_{b\lambda}$. But the weighting factor $p'_\lambda$ changes functional form with shift of $(x'_g,y'_g) = (\mu x_b,\mu y_b)$, and so Eq. (8) cannot be simplified by fourier transformation (ref. 4, pp. 40,108-110). In limited regions of the optical field, however, $p'_\lambda$ is almost a shift invariant function of the local coordinates,

$$\Delta x' = x'-x'_g = x'-\mu x_b \quad \text{and} \quad \Delta y' = y'-y'_g = y'-\mu y_b \quad [\text{cm}], \tag{9}$$

that is,

$$p'(x'_g,y'_g:x',y') \approx p'_\lambda(x'-\mu x_b,y'-\mu y_b) \quad [\text{cm}^{-2}]. \tag{10}$$

A region in which the point-spread function is adequately approximated by Eq. (10) is known as an isoplanatic patch (ref. 5; ref. 6, pp. 15-16, 19). In an isoplanatic patch the image spectral irradiance is given by

$$u'_\lambda(x',y') = \int_{-\infty}^{\infty}\int u_{b\lambda}\cdot p'_\lambda(x'-\mu x_b,y'-\mu y_b)\cdot dx_b dy_b \quad [\text{watts}/(\text{cm}^2\cdot\text{micron})]. \tag{11}$$

This is a 2-D convolution and so is reduced by fourier transformation to a simple product of two spectra. Thus, fourier analysis of an optical system is useful only in an isoplanatic patch. A large field of view may have to be divided into several isoplanatic patches to permit fourier analysis over the whole field.

The image can be blurred by atmospheric turbulence, aerosol scattering, and sensor motion as well as by optical aberration and diffraction. These effects can be accounted for at least approximately by including in the integrand of Eq. (11) other multiplicative terms like $p'_\lambda$ (ref. 7, §13.2; refs. 8-13). Such terms also may exhibit isoplanatic effects; that is, they may be approximately shift invariant only in limited regions of the optical field (ref. 14). For simplicity, factors representing additional blurring of the image are omitted here.

Eq. (11) is nevertheless inconvenient because it contains both object-plane and image-plane coordinates which differ in scale and orientation. This awkwardness can be eliminated by projecting the image plane onto the object plane under ideal conditions - gaussian optics, no atmospheric absorption or turbulence, no sensor motion, etc.. The projection is indicated in Fig. 1 by the ray from $(x',y')$ to $(x,y)$. In this way Eq. (11) becomes

$$u_\lambda(x,y) = \int_{-\infty}^{\infty}\int u_{b\lambda}\cdot p_\lambda(x-x_b,y-y_b)\cdot dx_b dy_b \quad [\text{watts}/(\text{cm}^2\cdot\text{micron})], \tag{12}$$

with $u_{b\lambda}$ given by Eq. (2a or b). Here $p_\lambda$ and $u_\lambda$ are the point-spread function and image irradiance expressed in object-plane quantities; $p_\lambda$ and $p'_\lambda$ have the same functional form, but $p_\lambda$ has units of reciprocal area in the object plane and is normalized so that $\int\int_{-\infty}^{\infty} p_\lambda \cdot dxdy = 1$. Also $p_\lambda = \mu^2 p'_\lambda$ since $p_\lambda \cdot dxdy$ must equal $p'_\lambda \cdot dx'dy'$. Henceforth all image-plane quantities are to be converted to object-plane quantities before substitution into the equations.

Two variations of the treatment above should be noted. First, Eq. (12) can be derived in fewer steps simply by reversing the directions of the image-plane axes in Fig. 1 and equating the magnification to unity at the outset (refs. 5,6). Though efficient, this befogs the physical meaning of the mathematics and the substitutions needed to obtain numerical results in actual cases. The derivation given here deals explicitly with these issues at the cost of lengthiness and a more elaborate notation than is essential. Second, some authors prefer the reverse of the projection employed here; that is, they project the object plane ideally onto the image plane and use Eqs. (3) and (4) to write Eq. (11) in terms of image-plane quantities (ref. 3, §§11-5,11-6; refs. 15,16). This is convenient if the problem being solved is in the image plane; Eq. (12) is more useful if the problem is in the object plane.

It is now necessary to examine the temporal dependence of Eq. (12) and its consequences more closely. With a scanning sensor, $u_{b\lambda} = u_{b\lambda}(x_b, y_b; T)$, and the convolution includes all variables. When the time and temporal-frequency variables are introduced later, they will merely replace x and the conjugate spatial-frequency variable $k_x$. Thus, no awkwardness will develop in the relations of either the space-time or the frequency domain. With a staring sensor, $u_{b\lambda} = u_{b\lambda}(x_b, y_b, t)$, and the convolution includes only two of the three variables. Time could be treated as a parameter and later regarded as a variable for describing analog processing, but this would make both the space-time and the frequency relations ungainly. A better alternative is to convolve Eq.(12) with a temporal delta function $\delta(t^*-t)$. In physical terms this selects image and object irradiances at a particular time $t^*$. But $t^*$ is continuously and arbitrarily assignable, so mathematically time remains a variable. This expedites fourier transformation and avoids the need to introduce time and temporal frequency as variables later. Thus, convenient image-irradiance functions for analysis of scanning and staring sensors are

$$\rightarrow u_\lambda(x,y,;T) = \int\int_{-\infty}^{\infty} u_{b\lambda}(x_b, y_b; T) \cdot p_\lambda(x-x_b, y-y_b) \cdot dx_b dy_b$$

$$= \theta_{a\lambda} \cdot \left[\theta_\lambda (A/d^2)\right] \cdot \int\int_{-\infty}^{\infty} n_{b\lambda} \cdot p_\lambda \cdot dx_b dy_b \ [\text{watts}/(\text{cm}^2 \cdot \text{micron})], \quad (13a)$$

and

$$\rightarrow u_\lambda(x,y,t^o) = \iiint_{-\infty}^{\infty} u_{b\lambda}(x_b,y_b,t)\cdot[p_\lambda(x-x_b,y-y_b)\cdot\delta(t^o-t)]\cdot dx_b dy_b dt$$

$$= \theta_{a\lambda}\cdot\left[\theta_\lambda(A/d^2)\right]\cdot\iiint_{-\infty}^{\infty} n_{b\lambda}\cdot[p_\lambda\cdot\delta]\cdot dx_b dy_b dt \ [\text{watts}/(\text{cm}^2\cdot\text{micron})]. \quad (13b)$$

B. Detector Response

Next consider the arbitrarily-shaped detector in Fig. 2 with center at $(x,y) = (x_c,y_c)$ and monochromatic responsivity $R_\lambda$, constant across the detector surface S. $R_\lambda$ will be expressed in (amps/watt) before measurement of response, but in (volts/watt) afterward, because detector current usually is measured by the voltage it produces across a capacitor. Image irradiance is assumed to vary slowly relative to detector-response time, so that the detector always responds fully to the illumination. The output from flux of wavelengths $\lambda$ to $(\lambda+d\lambda)$ is then

$$ds = R_\lambda\cdot d\lambda\cdot\iint_S u_\lambda\cdot dxdy \ \ [\text{amps}]. \quad (14)$$

Eq. (14) could be integrated over wavelength to find the total output, but it is convenient instead to define spectral output

$$\frac{ds}{d\lambda} = s_\lambda = R_\lambda\cdot\iint_S u_\lambda\cdot dxdy \ \ [\text{amps/micron}]. \quad (15)$$

Notation is now simplified by postponing the integration over wavelength until the final result is obtained.

Eq. (15), though correct, does not transform to a useful frequency-domain relation. A suitable alternative can be obtained, however, by inventing a detector-response function (Fig. 2) such that

$$\gamma(x_c-x,y_c-y) = 1 \ \text{ if } (x,y) \text{ is on the detector surface,}$$

$$= 0 \ \text{ elsewhere.} \quad (16)$$

With this function Eq. (15) becomes an easily transformable convolution:

$$s_\lambda(x_c,y_c) = R_\lambda\cdot\iint_{-\infty}^{\infty} u_\lambda(x,y)\cdot\gamma(x_c-x,y_c-y)\cdot dxdy \ \ [\text{amps/micron}]. \quad (17)$$

For the rectangular detector of width a and height b in Fig. 2, $\gamma$ is the product of two unit-amplitude rectangle functions (ref. 4, pp. 52,243):

$$\gamma = \mathrm{rect}\left(\frac{x_c-x}{a}\right)\cdot\mathrm{rect}\left(\frac{y_c-y}{b}\right)$$

$$= 1 \quad \text{if} \quad \left(x_c-\frac{a}{2}\right) < x < \left(x_c+\frac{a}{2}\right) \quad \text{and} \quad \left(y_c-\frac{b}{2}\right) < y < \left(y_c+\frac{b}{2}\right),$$

$$= 0 \quad \text{elsewhere.} \tag{18}$$

Response functions and their fourier transforms for some other detector shapes are given in reference 17, pp. 93-96. More generally, if the detector's responsivity varies across its surface, the variation can be included in $\gamma$; the tops of the functions in Fig. 2 then would be curved instead of flat. Since the detector is the field stop, it acts as the type of spatial filter called a reticle. Consequently, response functions for more complicated detector shapes and responsivities can be derived by reticle design-methods from specifications for the detector's spatial frequency response (ref. 18, pp. 485-502; refs. 19-22).

Eq. (17) with $u_\lambda = u_\lambda(x,y,;T)$ from Eq. (13b) approximates very nearly the momentary output of a detector whose field of view is swept over the background, provided the detector response-time is much less than the dwell time of an image point on the detector. Since additionally $u_\lambda$ is assumed constant during a scan, the time dependence of the output is easily formulated. With a constant scan rate $\zeta$ in the x direction, $x_c = x_o+\zeta t$ for a single scan. (For repeated scans the relation between $x_c$ and t is a sawtooth wave, and $u_\lambda$ is not independent of t; this case is not treated here.) Because Eq. (17) is shift invariant, the location of the origin is immaterial (ref. 3, pp. 108-110), allowing it to be chosen so that $x_o = 0$. The scanning detector output is then

$$\rightarrow s_\lambda(\zeta t,y_c) = R_\lambda\cdot\int_{-\infty}^{\infty}\int u_\lambda(x,y;T)\cdot\gamma(\zeta t-x,y_c-y)\cdot dxdy \quad \text{[amps/micron]}. \tag{19a}$$

Eq. (17) with $u_\lambda = u_\lambda(x,y,t^o)$ from Eq. (13a) also describes the time-dependent response of a detector whose field of view is fixed relative to the background. But the convolution of Eq. (17) involves only the two spatial variables, so as already explained an additional convolution with a temporal delta function is needed to avoid awkwardness in the equations. This gives for the output of a staring detector

$$\rightarrow s_\lambda(x_c,y_c,t) =$$

$$R_\lambda\cdot\int_{-\infty}^{\infty}\int\int u_\lambda(x,y,t^o)\cdot[\gamma(x_c-x,y_c-y)\cdot\delta(t-t^o)]\cdot dxdydt \quad \text{[amps/micron]}. \tag{19b}$$

Eq. (19a or b) represents the deterministic component of output from a detector whose center is located arbitrarily in space. The output also contains random components from temporal fluctuations of photon arrival at the detector and free charge in the detector. Only the deterministic component is considered in this work.

C. Analog Processing

If the detector output is sampled directly and instantaneously, Eqs. (19a and b) are suitable for constructing functions to represent sampled images. Before sampling, however, the output may pass through one or more stages of analog processing. As discussed later, the integration step of temporal-integral sampling usually can be treated as the final stage of such processing. Prior to that, the detector output often is sent through an analog low-pass or band-pass amplifier. This serves mainly to (1) raise the output well above any interference that might be picked up, (2) limit the dynamic range of the output, and (3) reduce aliasing by band limiting the random temporal frequencies.

It will be assumed that each stage of analog processing, including any temporal integration, is linear and shift invariant. The overall effect then can be described by a single impulse response $h(\tau)$, which is the convolution of the impulse responses of the stages. The processed detector output is the convolution of $h(\tau)$ with Eq. (19a or b). Neither of the latter convolutions involves the spatial variables. Thus, for reasons already explained, it is convenient to perform additional convolutions with one or two spatial delta functions. The processed outputs of scanning and staring sensors then are given by

$$\rightarrow s_{\lambda f}(\tau,\beta) = \iint_{-\infty}^{\infty} s_{\lambda}(\zeta t, y_c)\cdot[h(\tau-t)\cdot\delta(\beta-y_c)]\cdot dt dy_c \quad \left[\frac{\text{amps or volts}}{\text{micron}}\right], \quad (20a)$$

and

$$\rightarrow s_{\lambda f}(\alpha,\beta,\tau) =$$

$$\iiint_{-\infty}^{\infty} s_{\lambda}(x_c,y_c,t)\cdot[\delta(\alpha-x_c)\cdot\delta(\beta-y_c)\cdot h(\tau-t)]\cdot dx_c dy_c dt. \quad (20b)$$

The convolutions involving $h(\tau)$ are written in the usual way, so that $\tau$ is the continuous time at which the output occurs. Likewise $\alpha$ and $\beta$ are the detector-center coordinates of the analog-processed output and are continuous variables. If there is no analog processing, $h(\tau-t) = \delta(\tau-t)$. The temporal convolution of Eq. (20a) has a curious appearance because the argument of $s_{\lambda}$ is not t but position of the detector center $\zeta t = x_c$. Nevertheless, the integral correctly associates values of

$s_\lambda(\zeta t, y_c)$ with those of $h(\tau - t)$ and so gives the processed output correctly. The subscript f on the output symbols indicates filtering, which is appropriate since linear, shift-invariant processing has a filtering effect. The output units are [(amps or volts)/micron] depending on whether $R_\lambda$ in Eqs. (19a and b) has units of [(amps or volts)/watt].

D. Synopsis of Analog-Response Equations; the Pseudoimage

The equations for analog output have been derived by steps. At each step a function symbolizing a physical or experimental process was convolved with a function embodying the result of all prior processes. Thus the derivations can be summarized concisely by writing only the integrands and using the character • to indicate the integrations. With this notation the functions symbolizing the analog outputs of scanning and staring sensors are, respectively,

$$\rightarrow s_{\lambda f}(\tau,\beta;T)/R_\lambda = u_{b\lambda}(x_b,y_b;T) \bullet\bullet p_\lambda(x-x_b,y-y_b) \bullet\bullet r(\zeta t-x,y_c-y) \bullet\bullet [h(\tau-t)\cdot\delta(\beta-y_c)], \quad (21a)$$

and

$$\rightarrow s_{\lambda f}(\alpha,\beta,\tau)/R_\lambda = u_{b\lambda}(x_b,y_b,t) \bullet\bullet\bullet [p_\lambda(x-x_b,y-y_b)\cdot\delta(t^\bullet-t)] \bullet\bullet\bullet [r(x_c-x,y_c-y)\cdot\delta(t-t^\bullet)] \bullet\bullet\bullet [\delta(\alpha-x_c)\cdot\delta(\beta-y_c)\cdot h(\tau-t)]. \quad (21b)$$

(This notation differs from the usual one which employs asterisks and omits the integration variables, e.g., $z(x) = g(x)*w(x)$. Here the benefits of displaying the integration variables outweigh the liabilities of an unfamiliar notation. Reference 23 discusses deficiencies of the standard notation for use in optical analyses.)

By derivation Eq. (21a or b) represents analog-processed output from a single detector with center located arbitrarily in space. But since the detector center can be anywhere, Eq. (21a or b) gives the sensor output over all space. Thus $s_{\lambda f}$ can be regarded as a function describing a pseudoimage - the actual image blurred and otherwise altered by the detector and analog processing of its output. This interpretation is probably best for treating sampling and understanding the fourier spectrum of the sensor output. Typical units of $s_{\lambda f}$ are [volts/micron] when detector monochromatic responsivity $R_\lambda$ is expressed in [volts/watt]. The factors on the right sides of Eqs. (21a and b) are the apparent background spectral irradiance ($u_{b\lambda}$), the monochromatic point-spread function of the optics ($p_\lambda$), the detector-response function

($\gamma$), and the overall impulse response (h) for all stages of analog processing including, if applicable, the integration step of temporal-integral sampling. More explicit expressions for $u_{b\lambda}$ and $\gamma$ are given by Eqs. (2), (16), and (18). Eqs. (13a,b), (19a,b) and (20a,b) display the integral forms of the convolutions in Eqs. (21a,b).

## E. Sampling

For clarity, sampling will be described qualitatively before it is treated mathematically. Spatial sampling of an image can be implemented wholly or partly by arrays of photosensitive elements. As suggested by Fig. 3a, the elements of a staring array frequently are square and lie side by side in rows and columns. The elements of a scanning array (Fig. 3b) often are rectangular and are stacked in columns normal to the scan, with the centers of elements in adjacent columns staggered in the cross-scan direction. The cross-scan fields of view may be contiguous or overlap as in the figure. Each element may have its own amplifier, but if so the amplifiers have the same impulse response, so that the output in any channel is given by Eq. (21a or b).

Eqs. (15) and (17) show that the analog outputs result from spatial integration of image irradiance by the finite-size detector elements. Depending on the type of sensor, this represents partial or complete spatial integral-sampling of the image, which results in aliasing of image spatial-frequencies unless they are properly band limited (refs. 24,25; ref. 26, sec. 6.3.2; ref. 27, ch.9). With a staring sensor both the row (y) and column (x) spatial-frequency components can be aliased in the analog output because the detector geometry and mode of operation spatially sample the image in both directions. Consequently, with a staring sensor, spatial band-limiting can be achieved only by optical means (control of blur-circle and detector sizes). On the other hand, a scanning sensor spatially samples the image in the cross-scan (y) but not in the scan (x) direction. Thus, the cross-scan spatial-frequency components $k_y$ can be aliased in the analog output, but the co-scan components $k_x$ cannot be. In addition, scanning converts the x components to temporal frequencies which, assuming no lag in detector response, are given by $f = \zeta k_x$. It follows that the cross-scan spatial frequency components can be band limited only by optical means, but the co-scan components also can be band limited by sending the detector output through an analog amplifier. Ordinarily, however, filtering by the detector size attenuates the spatial frequencies far more.

An optical sensor's analog output usually is further sampled in time. This always involves charging a capacitor and, thus, temporal integration of charge, but the sampling is effectively instantaneous if the output and the sensor's field-of-view change little during sample measurement. In any case, the resulting samples may be assigned to

points of space and moments of time at the centers of the spatial and temporal integration intervals. Together, spatial and temporal sampling impose on the image a pattern of irradiance-integration areas and sample sites at intervals of $(\Delta x, \Delta y)$ as shown in Fig. 3. The sample sites are labeled by integers $(l,m)$ so that their coordinates are $(l\Delta x, m\Delta y)$. With a staring sensor, spatial and temporal sampling are independent. The integration areas are always identical to the detector-element areas and so cannot overlap (Fig. 3a). With a scanning sensor, spatial and temporal sampling are linked through scan rate $\zeta$, sampling duration $\varepsilon$, and sampling period $\Delta t \geq \varepsilon$. Temporal sampling induces spatial integral-sampling of the image in the scan direction and results in aliasing of the co-scan spatial-frequency components $k_x$ unless they have been band limited either optically or electronically. The integration areas exceed the detector-element area unless the detector moves little during sample measurement ($\zeta\varepsilon << a$). The integration areas can overlap, adjoin, or be separated in the scan direction depending on whether $(a+\zeta\varepsilon) >, =, < \zeta\Delta t$. Fig. 3b shows a case in which $(a+\zeta\varepsilon) > \zeta\Delta t$ and $\varepsilon < \Delta t$, so that the co-scan overlap $[a+\zeta(\varepsilon-\Delta t)]$ is $< a$. It should be noted that in Fig. 3b the offsets between the responses of detector elements in different columns have been removed to align the sample sites in the cross-scan direction. This can be done in one of three ways: by electronic delay before sampling; by making the ratio of column interval to sampling interval an integer and then shifting samples in different rows by the corresponding number of sites; or by interpolation of the sampled outputs. The second method is much the simplest in both practice and theory; the first is cumbersome to implement, and the third is equivalent to reconstructing the output.

(The type of sensor and sampling used in a particular case depend on the spatial and temporal coverage needed and certain engineering considerations. If the background or signal radiance changes during the scan time, a staring sensor must be used when temporal information is important, even though spatial information is lost between the integration areas. On the other hand, if the background and signal radiance are constant during the scan time, a scanning sensor is preferable since it allows complete spatial coverage and smaller spatial sampling intervals in both the scan and cross-scan directions. In practice, temporal integral-sampling usually is employed for surveillance, instantaneous sampling for data ollection. Charge from the detector of a surveillance sensor customarily is stored during successive time intervals of fixed duration, and the resulting sequence of charge packets is read out through a single lead. This procedure is followed because the detector commonly has too many photosensitive elements to permit a lead for each one. The detector of a data-collection sensor ordinarily has fewer elements, and temporal integration of the output is undesirable because it adds another instrumental effect to the data.)

The stage is now set for derivation of the 2-D sampling equations except for one item: Attention is directed to a lucid graphical and algebraic treatment of temporal sampling in chapters 5 and 6 of reference 28, and to a brief overview of 2-D spatial sampling in section 6.3.1 of reference 26. Anyone who has trouble following the derivations below should first study these sources.

Sampling of a temporal wavefrom is most often treated as amplitude modulation of a pulse-train carrier by the waveform; that is, the process is represented mathematically by a product of carrier and waveform functions. The carrier pulses usually are identical, equally spaced, and rectangular. Other kinds of sampling are possible, but this is the most common type. Sampling ordinarily is followed by holding, quantization, and encoding of the sample values. (Ref. 29, §§2.4,2.6) The present treatment is limited to the most common type of sampling with no consideration of the last three steps.

For "instantaneous" sampling the pulse width (sampling duration $\varepsilon$) is less than both the time between pulses (sampling period $\Delta t$) and the least time constant of the waveform. The carrier then can be approximated mathematically by a comb distribution (ref. 29, pp. 52-59; ref. 3, §3.2):

$$\frac{\mathrm{comb}(t/\Delta t)}{|\Delta t|} = \sum_{n=-\infty}^{\infty} \delta(t-n\Delta t) \quad [\mathrm{sec}^{-1}] \tag{22}$$

To sample the multiple outputs of an electro-optical sensor, there must be a pulse train at the position of each output. With a scanning sensor this requires a pulse train at the cross-scan position of each detector element. The carrier function for instantaneous sampling during a single scan can be written as the product of a temporal and a cross-scan spatial comb (ref. 3, §3.4):

$$\frac{\mathrm{comb}(\tau/\Delta t)}{|\Delta t|}\cdot\frac{\mathrm{comb}(\beta/\Delta y)}{|\Delta y|} = \sum_{l=-\infty}^{\infty} \delta(\tau-l\Delta t)\cdot\sum_{m=-\infty}^{\infty} \delta(\beta-m\Delta y) \quad [(\mathrm{cm}\cdot\mathrm{sec})^{-1}]. \tag{23a}$$

The time variable is represented by $\tau$ to agree with Eq. (21a). In Eq. (22) "n" is the temporal summation index; in Eq. (23a) "l" is used instead to indicate the equivalence of time and position in the scan (x) direction. Eq (23a) tacitly represents a 2-D spatial array of impulses that are deployed column-by-column at intervals of $\Delta x = \zeta\Delta t$ during a scan. Because the time $\Delta T$ between images must be at least as great as the scan time, it is necessary that $\Delta T \geq (l-1)\Delta t$, where l is the number of columns in the impulse array. Thus Eq. (23a) is limited to one scan; it cannot be used in representing a sequence of images from successive scans, a problem not treated here.

The carrier function for instantaneous sampling of a staring sensor's output is effectively a temporal sequence of impulse arrays. It can be written as the product of a temporal comb with two spatial combs:

$$\frac{\mathrm{comb}(\alpha/\Delta x)}{|\Delta x|}\cdot\frac{\mathrm{comb}(\beta/\Delta y)}{|\Delta y|}\cdot\frac{\mathrm{comb}(\tau/\Delta T)}{|\Delta T|} \qquad [(\mathrm{cm}^2\cdot\mathrm{sec})^{-1}]$$

$$= \sum_{l=-\infty}^{\infty}\delta(\alpha-l\Delta x)\cdot\sum_{m=-\infty}^{\infty}\delta(\beta-m\Delta y)\cdot\sum_{n=-\infty}^{\infty}\delta(\tau-n\Delta T). \quad (23b)$$

$\Delta T$ is both the sampling period and the time between sampled images (also called data frames), so that the epoch of an image is $T = n\Delta T$.

An instantaneously sampled image from a scanning sensor is now represented by the product of Eq. (21a) for the analog output and Eq. (23a) for the sampling carrier:

$$\rightarrow (\grave{dv}/d\lambda)_f \equiv \grave{v}_{\lambda f}(\tau,\beta;T) \qquad [\mathrm{volts}/(\mathrm{micron}\cdot\mathrm{cm}\cdot\mathrm{sec})]$$

$$= s_{\lambda f}(\tau,\beta;T)\cdot\left[\sum_{l=-\infty}^{\infty}\delta(\tau-l\Delta t)\cdot\sum_{m=-\infty}^{\infty}\delta(\beta-m\Delta y)\right]$$

$$= \sum_{l,m=-\infty}^{\infty}\sum s_{\lambda f}(l\Delta t,m\Delta y;T)\cdot\left[\delta(\tau-l\Delta t)\cdot\delta(\beta-m\Delta y)\right]. \quad (24a)$$

The grave accents $\grave{}$ denote sampled quantities; the last equality follows from the relation $g(x)\cdot\delta(x-a) = g(a)\cdot\delta(x-a)$; and the voltage unit indicates units of (volts/watt) for $R_\lambda$ in Eq. (21a). With a staring sensor Eq. (21b) represents the analog output and Eq. (23b) the carrier, so that the instantaneously sampled image is symbolized by

$$\rightarrow (\grave{dv}/d\lambda)_f \equiv \grave{v}_{\lambda f}(\alpha,\beta,\tau) \qquad [\mathrm{volts}/(\mathrm{micron}\cdot\mathrm{cm}^2\cdot\mathrm{sec})]$$

$$= s_{\lambda f}(\alpha,\beta,\tau)\cdot\left[\sum_{l=-\infty}^{\infty}\delta(\alpha-l\Delta x)\cdot\sum_{m=-\infty}^{\infty}\delta(\beta-m\Delta y)\cdot\sum_{n=-\infty}^{\infty}\delta(\tau-n\Delta T)\right]$$

$$= \sum_{l,m,n=-\infty}^{\infty}\sum\sum s_{\lambda f}(l\Delta x,m\Delta y,n\Delta T)\cdot\left[\delta(\alpha-l\Delta x)\cdot\delta(\beta-m\Delta y)\cdot\delta(\tau-n\Delta T)\right]. \quad (24b)$$

It should be noted that $\grave{v}_{\lambda f}(\tau,\beta;T)$ and $\grave{v}_{\lambda f}(\alpha,\beta,\tau)$ are distributions (generalized functions); they are not arrays of sample values, which are obtained by integration of Eqs. (24a and b). For example, the (l,m,n)th sample value is obtained from Eq. (24b) by integration between the limits $[(l\pm c)\Delta x,(m\pm c)\Delta y,(n\pm c)\Delta t]$ with $0 < c < 1$.

As already mentioned, sampling in operational sensors usually is not instantaneous. Rather, the sampling duration is a significant fraction of the sampling interval and the least time constant of the waveform being sampled. This is called finite-pulse-width or temporal-integral sampling. The reason for the latter name will soon appear. A rigorous treatment of temporal-integral sampling is not simple, and the results are circuit-dependent (ref. 29, §2.7; ref. 30, ch. 9; ref. 31, ch.

11; refs. 32-37). However, the following heuristic treatment is valid for the most commonly used circuits. After modulation the tops of the carrier pulses ideally have the shape of the modulating waveform in the sampling durations. (Hence the modulation process also is called waveform chopping.) To obtain measures of the waveform amplitude, the modulated pulse heights must be averaged over the pulse width. This can be done by convolving the pulses with a unit-area rectangle function having width $\varepsilon$ and, for causality, center $(\varepsilon/2)$:

$$\frac{1}{\varepsilon}\mathrm{rect}\left[\frac{\tau-(\varepsilon/2)}{\varepsilon}\right] = 1 \quad \text{if} \quad 0 < t < \varepsilon,$$

$$= 0 \quad \text{elsewhere.} \tag{25}$$

But the same result must be obtained if first the sensor output is convolved with the rectangle function, and then the time-averaged waveform is sampled instantaneously at times corresponding to the trailing pulse edges. Thus the most common integral samplers are equivalent to a linear filter (integrator) followed by an instantaneous sampler (ref. 29, p. 42; ref. 3, pp. 283-285; refs. 36-37).

For simplicity, temporal integration of sensor output is included in the overall impulse response for analog processing. In other words, Eqs. (21a and b) represent temporally averaged or unaveraged waveforms depending on whether $h(\tau)$ includes the equivalent impulse response of a temporal-integral sampler. Consequently, Eqs. (24a and b) are easily modified to represent integrally sampled images; with temporal averaging indicated by angular brackets $\langle\ \rangle$, the relations for scanning and staring sensors are

$$\langle v'_{\lambda f}(\tau,\beta;T)\rangle \quad [\text{volts}/(\text{micron}\cdot\text{cm}\cdot\text{sec})]$$

$$= \langle s_{\lambda f}(\tau,\beta;T)\rangle \cdot \left[\sum_{l=-\infty}^{\infty} \delta(\tau-l\Delta t)\cdot \sum_{m=-\infty}^{\infty} \delta(\beta-m\Delta y)\right]$$

$$= \sum_{l,m=-\infty}^{\infty}\sum \langle s_{\lambda f}(l\Delta t, m\Delta y;T)\rangle \cdot \left[\delta(\tau-l\Delta t)\cdot\delta(\beta-m\Delta y)\right]. \tag{26a}$$

and

$$\langle v'_{\lambda f}(\alpha,\beta,\tau)\rangle \quad [\text{volts}/(\text{micron}\cdot\text{cm}^2\cdot\text{sec})]$$

$$= \langle s_{\lambda f}(\alpha,\beta,\tau)\rangle \cdot \left[\sum_{l=-\infty}^{\infty} \delta(\alpha-l\Delta x)\cdot \sum_{m=-\infty}^{\infty} \delta(\beta-m\Delta y)\cdot \sum_{n=-\infty}^{\infty} \delta(\tau-n\Delta T)\right]$$

$$= \sum_{l,m,n=-\infty}^{\infty}\sum\sum \langle s_{\lambda f}(l\Delta x, m\Delta y, n\Delta T)\rangle \cdot \left[\delta(\alpha-l\Delta x)\cdot\delta(\beta-m\Delta y)\cdot\delta(\tau-n\Delta T)\right]. \tag{26b}$$

Use of a rectangle function for waveform averaging assumes that the sampling circuit forms an unweighted average of the pulse height. If

not, the rectangle function is simply replaced by the correct weighting function, which is the equivalent-circuit impulse response normalized to have unit area. This is similar to inclusion of nonuniform detector responsivity in the detector-response function Eq. (16). With a scanning sensor, temporal averaging of pulse height results in the irradiance-integration areas of Fig 3b. This is physically obvious and follows from Eq. (21a) and the commutative property of convolution. Thus the treatments of spatial-integral and temporal-integral sampling are analogous and consistent.

Fig. 3 and the discussion above indicate that scanning and temporal integration effectively reduce spatial resolution and detector responsivity. Resolution is reduced because the integration area exceeds the detector-element area. Responsivity is decreased because at any time the detector element occupies only a fraction of the integration area, whereas it always would occupy the whole area if the sensor were staring.

Finally, it should be noted that neither instantaneous nor integral sampling is shift invariant. The waveform-averaging step of integral sampling is, but the instantaneous-sampling step is not. The sample values depend on the phase between the comb function and the waveform being sampled. This is important at low sampling rates.

## F. Image Cropping

To obtain finite arrays of samples for recording, the images and image sequences must be truncated. This is done physically by truncating the carrier before modulation (ref. 3, p. 278), but the order of the operations is mathematically reversible because the result is expressed by an associative and commutative product of functions.

The cropping or truncating function for one image from a scanner is a product of two unit-amplitude rectangle functions that select M rows of the image and L samples in each row. For computation it is desirable to have the summation indices of the cropped image function begin with zero. This is accomplished as shown in Fig. 4 by placing the lower edge of each rectangle function one-half sampling period below the coordinate origin. The cropping or truncating function now can be written

$$\operatorname{crop}(\tau,\Delta t,L{:}\beta,\Delta y,M) = \operatorname{rect}\left[\frac{\tau-(L-1)(\Delta t/2)}{L\Delta t}\right]\cdot\operatorname{rect}\left[\frac{\beta-(M-1)(\Delta y/2)}{M\Delta y}\right]$$

$$= 1 \quad \text{if } \left(\frac{-\Delta t}{2}\right) < \tau < \left(L-\frac{1}{2}\right)\Delta t \quad \text{and} \quad \left(\frac{-\Delta y}{2}\right) < \beta < \left(M-\frac{1}{2}\right)\Delta y;$$

$$= 0 \quad \text{elsewhere.} \qquad (27a)$$

Eq. (27a) is easily extended to obtain a function that acts on the sampled output of a staring sensor to select and crop the image with epoch $T = 0$. Recalling that $\tau$ and $x$ are equivalent in Eq. (27a) and that $T = n\Delta T$, one sees that the desired function is

$$\begin{aligned}
&\text{crop}(\alpha,\Delta x,L{:}\beta,\Delta y,M{:}\tau,\Delta T)\\
&\quad = \text{rect}\left[\frac{\alpha-(L-1)(\Delta x/2)}{L\Delta x}\right]\cdot\text{rect}\left[\frac{\beta-(M-1)(\Delta y/2)}{M\Delta y}\right]\cdot\text{rect}[\tau/\Delta T]\\
&\quad = 1 \quad \text{if} \quad \left(\frac{-\Delta x}{2}\right) < \alpha < \left(L-\frac{1}{2}\right)\Delta x, \quad \left(\frac{-\Delta y}{2}\right) < \beta < \left(M-\frac{1}{2}\right)\Delta y,\\
&\qquad\qquad \text{and } (-\Delta T/2) < \tau < (\Delta T/2);\\
&\quad = 0 \quad \text{elsewhere.}
\end{aligned} \tag{27b}$$

Cropped images are represented by the products of Eqs. (27a,b) with Eqs. (24a,b) and (26a,b). Thus, with $\backslash\ \backslash$ denoting truncation, instantaneously sampled and cropped images with epoch $T = 0$ are, for a scanning sensor,

$$\begin{aligned}
&\rightarrow \backslash\dot{v}_{\lambda f}(\tau,\beta;T=0)\backslash \quad [\text{volts}/(\text{micron}\cdot\text{cm}\cdot\text{sec})]\\
&\quad = \dot{v}_{\lambda f}(\tau,\beta;T=0)\cdot\text{rect}\left[\frac{\tau-(L-1)(\Delta t/2)}{L\Delta t}\right]\cdot\text{rect}\left[\frac{\beta-(M-1)(\Delta y/2)}{M\Delta y}\right]\\
&\quad = \sum_{l=0}^{(L-1)}\sum_{m=0}^{(M-1)} s_{\lambda f}(l\Delta t,m\Delta y;T=0)\cdot[\delta(\tau-l\Delta t)\cdot\delta(\beta-m\Delta y)],
\end{aligned} \tag{28a}$$

and for a staring sensor,

$$\begin{aligned}
&\rightarrow \backslash\dot{v}_{\lambda f}(\alpha,\beta,\tau)\backslash \quad [\text{volts}/(\text{micron}\cdot\text{cm}^2\cdot\text{sec})]\\
&\quad = \dot{v}_{\lambda f}(\alpha,\beta,\tau)\cdot\text{rect}\left[\frac{\alpha-(L-1)(\Delta x/2)}{L\Delta x}\right]\cdot\text{rect}\left[\frac{\beta-(M-1)(\Delta y/2)}{M\Delta y}\right]\cdot\text{rect}[\tau/\Delta T]\\
&\quad = \sum_{l=0}^{(L-1)}\sum_{m=0}^{(M-1)} s_{\lambda f}(l\Delta x,m\Delta y;T=0)\cdot[\delta(\alpha-l\Delta x)\cdot\delta(\beta-m\Delta y)\cdot\delta(\tau)].
\end{aligned} \tag{28b}$$

The corresponding integrally sampled and cropped images from scanning and staring sensors are

$$\begin{aligned}
&\backslash\langle\dot{v}_{\lambda f}(\tau,\beta;T=0)\rangle\backslash \quad [\text{volts}/(\text{micron}\cdot\text{cm}\cdot\text{sec})]\\
&\quad = \langle\dot{v}_{\lambda f}(\tau,\beta;T=0)\rangle\cdot\text{rect}\left[\frac{\tau-(L-1)(\Delta t/2)}{L\Delta t}\right]\cdot\text{rect}\left[\frac{\beta-(M-1)(\Delta y/2)}{M\Delta y}\right]\\
&\quad = \sum_{l=0}^{(L-1)}\sum_{m=0}^{(M-1)} \langle s_{\lambda f}(l\Delta t,m\Delta y;T=0)\rangle\cdot[\delta(\tau-l\Delta t)\cdot\delta(\beta-m\Delta y)],
\end{aligned} \tag{29a}$$

and

$$\begin{aligned}
&\backslash\langle\dot{v}_{\lambda f}(\alpha,\beta,\tau)\rangle\backslash \quad [\text{volts}/(\text{micron}\cdot\text{cm}^2\cdot\text{sec})]\\
&\quad = \langle\dot{v}_{\lambda f}(\alpha,\beta,\tau)\rangle\cdot\text{rect}\left[\frac{\alpha-(L-1)(\Delta x/2)}{L\Delta t}\right]\cdot\text{rect}\left[\frac{\beta-(M-1)(\Delta y/2)}{M\Delta y}\right]\cdot\text{rect}[\tau/\Delta T]
\end{aligned}$$

(Continues)

$$= \sum_{l=0}^{(L-1)} \sum_{m=0}^{(M-1)} \langle s_{\lambda f}(l\Delta x, m\Delta y; T=0)\rangle \cdot [\delta(\alpha - l\Delta x)\cdot\delta(\beta - m\Delta y)\cdot\delta(\tau)]. \qquad (29b)$$

## III. FREQUENCY-DOMAIN DERIVATIONS

Frequency-domain equations are obtained simply by taking fourier transforms of space- and time-domain equations. For this purpose, certain definitions and mathematical relations are needed.

The fourier transform has been defined in at least six ways differing in normalization constant and sign of exponent. In addition, both members of a transform pair have been called the inverse by different authors. The conventions and notation used here are, for the transform,

$$G(k_x,k_y,f) \equiv {}^{3}F[g(x,y,t)] \equiv \iiint_{-\infty}^{\infty} g\cdot\exp[-i2\pi(k_x x+k_y y+ft)]\cdot dxdydt, \qquad (30)$$

and for its inverse,

$${}^{-3}F[G(k_x,k_y,f)] \equiv \iiint_{-\infty}^{\infty} G\cdot\exp[i2\pi(k_x x+k_y y+ft)]\cdot dk_x dk_y df = g(x,y,t). \qquad (31)$$

A space-time function and its transform are denoted, respectively, by the small and capital forms of a letter. The operator symbols ${}^{3}F[\ ]$ and ${}^{-3}F[\ ]$ are explained by the integrals. In these relations $i = \sqrt{(-1)}$; $(x,y,t)$ and $(k_x,k_y,f)$ are sets of independent, orthogonal coordinates consisting of pairs of conjugates $(x,k_x)$, $(y,k_y)$, $(t,f)$; f is temporal frequency; and $(k_x,k_y)$ are the magnitudes of the components of the spatial frequency vector $\hat{k} = \hat{k}_x+\hat{k}_y$. The unit of f adopted is the (cycle/sec) or hertz (hz). Common units of $\hat{k}$ are the (cycle/cm) and (cycle/mr), which also are called the reciprocal centimeter (rcm) and reciprocal milliradian (rmr). The former is used here. Spatial frequencies in the object and image planes are related by $\hat{k} = \mu\hat{k}'$, but this relation is not needed here since all quantities are measured in the object plane.

With a staring sensor there are no constraints among the coordinates. All are independent and can be treated as variables or parameters. Eqs. (30) and (31) then allow three-, two-, and one-dimensional transforms. Examples of the latter types are

$${}^{2}F[g(x,y;t)] = G(k_x,k_y;t), \qquad {}^{1}F[g(t;x,y)] = G(f;x,y),$$
$${}^{-2}F[G(k_x,k_y;f)] = g(x,y;f), \qquad {}^{-1}F[G(f;k_x,k_y) = g(t;k_x,k_y).$$

Scanning introduces the constraints $x_c = \zeta t$ and $f = \zeta k_x$, which rule out 3-D transforms. The choices of independent, conjugate coordinates are $(y,k_y)$ and either $(x,k_x)$ or $(t,f)$. Eqs. (30) and (31) give different 2-D transform pairs depending on the choice. Consequently, the scaling relations between the results in the two cases are required. These are well known but are displayed below for ease of reference.

$$ {}^{2}\mathcal{F}[g(x,y)] \equiv \int_{-\infty}^{\infty}\int g\cdot\exp[-i2\pi(k_x x+k_y y)]\cdot dxdy \equiv G(k_x,k_y) = G(f/\zeta,k_y) \qquad (32) $$

$$ {}^{2}\mathcal{F}[g(\zeta t,y)] \equiv \int_{-\infty}^{\infty}\int g\cdot\exp[-i2\pi(ft+k_y y)]\cdot dtdy = \frac{1}{\zeta}\cdot G(k_x,k_y) = \frac{1}{\zeta}\cdot G(f/\zeta,k_y) \qquad (33) $$

$$ {}^{-2}\mathcal{F}[G(k_x,k_y)] \equiv \int_{-\infty}^{\infty}\int G\cdot\exp[i2\pi(k_x x+k_y y)]\cdot dk_x dk_y = g(x,y) \qquad (34) $$

$$ {}^{-2}\mathcal{F}[G(f/\zeta,k_y)] \equiv \int_{-\infty}^{\infty}\int G\cdot\exp[i2\pi(ft+k_y y)]\cdot dfdk_y = \zeta\cdot g(x,y) = \zeta\cdot g(\zeta t,y) \qquad (35) $$

Two versions of the convolution theorem are needed. They are derived in references 3 (p. 196) and 38 (p. 57) for one variable; derivations for two and three variables are easily developed from these examples, as in appendices A and B. One version of the theorem says that the transform of a convolution is the product of the transforms of the convolved functions. Because a variety of functions have been convolved in Part II, this version is needed in all the guises below. For the scanning cases it is also desirable to express the different forms in terms of the two equivalent frequencies $k_x$ and $f$.

$$ {}^{2}\mathcal{F}[g(x^o,y^o)\bullet\bullet w(x-x^o,y-y^o)] = G(k_x,k_y)\cdot W(k_x,k_y) = G(f/\zeta,k_y)\cdot W(f/\zeta,k_y) \qquad (36a) $$

$$ {}^{2}\mathcal{F}[g(x,y)\bullet\bullet w(\zeta t-x,y^o-y)] = G(k_x,k_y)\cdot\frac{1}{\zeta}W(k_x,k_y) = G(f/\zeta,k_y)\cdot\frac{1}{\zeta}W(f/\zeta,k_y) \qquad (36a') $$

$$ {}^{2}\mathcal{F}\{g(\zeta t,y^o)\bullet\bullet[q(t^o-t)\cdot w(y-y^o)]\} = \frac{1}{\zeta}G(k_x,k_y)\cdot Q(\zeta k_x)\cdot W(k_y) = \frac{1}{\zeta}G(f/\zeta,k_y)\cdot Q(f)\cdot W(k_y) \qquad (36a'') $$

$$ {}^{3}\mathcal{F}\{g(x,y,t)\bullet\bullet\bullet[q(x^o-x,y^o-y)\cdot w(t^o-t)]\} = G(k_x,k_y,f)\cdot Q(k_x,k_y)\cdot W(f) \qquad (36b) $$

$$ {}^{3}\mathcal{F}\{g(x^o,y^o,t)\bullet\bullet\bullet[q(x-x^o)\cdot w(y-y^o)\cdot z(t^o-t)]\} = G(k_x,k_y,f)\cdot Q(k_x)\cdot W(k_y)\cdot Z(f) \qquad (36b') $$

A second version of the theorem says that the transform of a product is the convolution of the transforms of the factors. Symbolically,

$$^3F\{g(x,y,t)\cdot[q(x)\cdot w(y)\cdot z(t)]\}$$
$$= G(k_x^\circ,k_y^\circ,f^\circ)\circledast Q(k_x-k_x^\circ)\circledast W(k_y-k_y^\circ)\circledast Z(f-f^\circ) \quad (37)$$

Eq. (37) suffices with this version because it is never necessary to transform products with factors different from those shown, and because the 2-D equation is obtained by omitting x components from Eq. (37).

The transform definitions and convolution theorems are expressed in terms of the general space-time coordinates (x,y,t). In applying these relations one must recall distinctions already made between (x,y,t) and other associated coordinates. For example, $(x_c,y_c)$ are the spatial coordinates of the detector center, and $(\alpha,\beta)$ are the central coordinates of the spatial integration intervals. Also the space-time scanning constraint is $x_c = \zeta t$, not $x = \zeta t$. But there are no such distinctions between the frequency coordinates; $(k_x,k_y,f)$ are conjugate to any of the respective space-time coordinates, and the scanning constraint for frequencies is $f = \zeta k_x$ regardless of the space-time coordinates.

Frequency-domain equations are now derived by straightforward but tedious application of the transform definitions and convolution theorems to the space- and time-domain results. Subsection IID summarizes the analog frequency-domain equations and provides an overview which cuts through the details of their derivation.

A. Fourier Spectra of Object and Image

From Eq. (30) the fourier spectra of the object radiance for treatment of scanning and staring sensors are

$$N_{b\lambda}(k_x,k_y;T) = {}^2F[n_{b\lambda}(x_b,y_b;T)] \quad [\text{watts}/(\text{cm}^2\cdot\text{str}\cdot\text{micron}\cdot\text{rcm}^2)] \quad (38a)$$

and

$$N_{b\lambda}(k_x,k_y,f) = {}^3F[n_{b\lambda}(x_b,y_b,t)] \quad [\text{watts}/(\text{cm}^2\cdot\text{str}\cdot\text{micron}\cdot\text{rcm}^2\cdot\text{hz})]. \quad (38b)$$

Transformation of Eqs. (2a and b) according to Eqs. (32) and (30) gives the spectra of the apparent object irradiances in the two cases:

$$U_{b\lambda}(k_x,k_y;T) = {}^2F[u_{b\lambda}(x_b,y_b;T)] \quad [\text{watts}/(\text{cm}^2\cdot\text{micron}\cdot\text{rcm}^2)]$$
$$= \theta_{a\lambda}\cdot\left[\theta_\lambda(A/d^2)\right]\cdot N_{b\lambda}(k_x,k_y;T) = \theta_{a\lambda}\cdot\left[\theta_\lambda(A/d^2)\right]\cdot N_{b\lambda}(f/\zeta,k_y;T); \quad (39a)$$

$$U_{b\lambda}(k_x,k_y,f) = {}^3F[u_{b\lambda}(x_b,y_b,t)]$$
$$= \theta_{a\lambda}\cdot\left[\theta_\lambda(A/d^2)\right]\cdot N_{b\lambda}(k_x,k_y,f) \quad [\text{watts}/(\text{cm}^2\cdot\text{micron}\cdot\text{rcm}^2\cdot\text{hz})]. \quad (39b)$$

Fourier spectra of the image irradiances are obtained by transformation of Eqs. (13a and b) using Eq. (30) and the convolution theorems of Eqs. (36a and b):

$$U_\lambda(k_x,k_y;T) = {}^2F[u_\lambda(x,y;T)] \qquad [\text{watts}/(\text{cm}^2\cdot\text{micron}\cdot\text{rcm}^2)]$$

$$= {}^2F[u_{b\lambda}(x_b,y_b;T)\bullet\bullet p_\lambda(x-x_b,y-y_b)]$$

$$= U_{b\lambda}(k_x,k_y;T)\cdot P_\lambda(k_x,k_y) = U_{b\lambda}(f/\zeta,k_y;T)\cdot P_\lambda(f/\zeta,k_y) \qquad (40a)$$

$$U_\lambda(k_x,k_y,f) = {}^3F[u_\lambda(x,y,t)]$$

$$= {}^3F\{u_{b\lambda}(x_b,y_b,t)\bullet\bullet\bullet[p_\lambda(x-x_b,y-y_b)\cdot\delta(t^o-t)]\}$$

$$= U_{b\lambda}(k_x,k_y,f)\cdot P_\lambda(k_x,k_y) \quad [\text{watts}/(\text{cm}^2\cdot\text{micron}\cdot\text{rcm}^2\cdot\text{hz})] \qquad (40b)$$

Since $u_\lambda$ is image irradiance projected ideally onto the object plane, all quantities in Eqs. (40a and b) are to be measured in the object plane.

The factor $P_\lambda$ in these equations is the fourier transform of the point-spread function:

$$P_\lambda(k_x,k_y) = {}^2F[p_\lambda(x-x_b,y-y_b)] \quad [\text{dimensionless}] \qquad (41)$$

If $p_\lambda$ is approximated by a circular gaussian function,

$$P_\lambda(k_x,k_y) = {}^2F\{c^{-2}\cdot\exp[-\pi(x-x_b)^2/c^2]\cdot\exp[-\pi(y-y_b)^2/c^2]\}$$

$$= \exp[-\pi c^2(k_x^2+k_y^2)]. \qquad (42)$$

Eqs. (42) and (40a,b) indicate that the optics filter the object spectrum, as follows. The parameter c, which is a measure of the blur circle size, governs the variation of the gaussian functions. If the blur circle is large, $P_\lambda$ decreases rapidly with increase of $(k_x^2+k_y^2)$, and the high spatial frequencies of $U_{b\lambda}$ are strongly attenuated. For high resolution (reproduction of fine detail) the blur circle must be small, i.e., the optics must pass high spatial frequencies. By analogy to electrical filters, $P_\lambda$ is called the optical transfer function. Reference 39 is a thorough and readable account of this function's properties, measurement, computation, and uses.

## B. Fourier Spectra of Detector Response

Application of Eqs. (33) and (36a') to Eq. (19a) for a scanning detector's output gives for the spectrum

$$
\begin{aligned}
{}^{2}F[s_\lambda(\zeta t, y_c; T)] &= R_\lambda \cdot {}^{2}F[u_\lambda(x,y;T) \overset{\bullet\bullet}{} \gamma(\zeta t - x, y_c - y)] \quad [\text{amps}/(\text{micron}\cdot\text{rcm}\cdot\text{hz})] \\
&= \tfrac{1}{\zeta} S_\lambda(k_x, k_y; T) = (R_\lambda/\zeta)\cdot U_\lambda(k_x, k_y; T)\cdot\Gamma(k_x, k_y) \\
&= \tfrac{1}{\zeta} S_\lambda(f/\zeta, k_y; T) = (R_\lambda/\zeta)\cdot U_\lambda(f/\zeta, k_y; T)\cdot\Gamma(f/\zeta, k_y). \qquad (43a)
\end{aligned}
$$

Similarly, applying Eqs. (30) and (36b) to Eq. (19b), one finds for the spectrum of a staring detector's output

$$
\begin{aligned}
S_\lambda(k_x, k_y, f) &\equiv {}^{3}F[s_\lambda(x_c, y_c, t)] \\
&= R_\lambda \cdot {}^{3}F\{u_\lambda(x,y,t^\circ) \overset{\bullet\bullet\bullet}{} [\gamma(x_c - x, y_c - y)\cdot\delta(t - t^\circ)]\} \\
&= R_\lambda \cdot U_\lambda(k_x, k_y, f)\cdot\Gamma(k_x, k_y) \quad [\text{amps}/(\text{micron}\cdot\text{rcm}^2\cdot\text{hz})]. \qquad (43b)
\end{aligned}
$$

In these equations $S_\lambda$ is the spectrum of the output from a single detector element arbitrarily located in space. $\Gamma(k_x, k_y)$ is the fourier transform of the detector-response function Eq. (16):

$$
\Gamma(k_x, k_y) \equiv {}^{2}F[\gamma(x_c - x, y_c - y)] \quad [\text{cm}^2 \text{ or } \text{rcm}^{-2}] \qquad (44)
$$

If the detector is rectangular, $\gamma$ is given by Eq. (18) and

$$
\Gamma(k_x, k_y) = [a\cdot\text{sinc}(k_x a)\cdot\exp(-i2\pi k_x x_c)]\cdot[b\cdot\text{sinc}(k_y b)\cdot\exp(-i2\pi k_y y_c)], \qquad (45)
$$

where $\text{sinc}(k_x a) = (\sin \pi k_x a)/\pi k_x a$. Eqs. (45) and (43) show that, like the optics, the detector filters spatial frequencies. Hence $\Gamma$ is called the detector transfer function. As the detector width (a) and height (b) are increased, the first zeros of the sinc functions occur at lower values of $k_x$ and $k_y$, resulting in greater attenuation of higher spatial frequencies in the image spectra $U_\lambda$. The detector usually attenuates the spatial frequencies more than any other sensor component.

## C. Pseudoimage Spectra

Eq. (20a) for the analog output of a scanning sensor is transformed with the aid of Eqs. (30) and (36a") to obtain

$$
\begin{aligned}
S_{\lambda f}(f, k_y; T) &\equiv {}^{2}F[s_{\lambda f}(\tau, \beta; T)] \qquad [(\text{amps or volts})/(\text{micron}\cdot\text{rcm}\cdot\text{hz})] \\
&= {}^{2}F\{s_\lambda(\zeta t, y_c; T) \overset{\bullet\bullet}{} [h(\tau - t)\cdot\delta(\beta - y_c]\} \\
&= \tfrac{1}{\zeta} S_\lambda(k_x, k_y)\cdot H(\zeta k_x) = \tfrac{1}{\zeta} S_\lambda(f/\zeta, k_y; T)\cdot H(f). \qquad (46a)
\end{aligned}
$$

Using Eqs. (30) and (36b') to transform Eq. (20b) for a staring sensor's analog output gives

$$S_{\lambda f}(k_x,k_y,f) \equiv {}^3\mathcal{F}[s_{\lambda f}(\alpha,\beta,\tau)] \qquad [(\text{amps or volts})/(\text{micron}\cdot\text{rcm}^2\cdot\text{hz})]$$

$$= {}^3\mathcal{F}\{s_\lambda(x_c,y_c,t)\bullet\bullet\bullet[\delta(\alpha-x_c)\cdot\delta(\beta-y_c)\cdot h(\tau-t)]\}$$

$$= S_\lambda(k_x,k_y,f)\cdot H(f). \qquad (46b)$$

H(f) is the transfer function for all analog processing of a detector element's output including, if applicable, the integration step of temporal-integral sampling. $S_{\lambda f}$ is the spectrum of analog-processed output from a detector element located anywhere in space, or it is the spectrum of a pseudoimage, as explained in the next subsection. The units of $S_{\lambda f}$ (amps or volts) are determined by the units of $R_\lambda$ (amps or volts/watt) in Eqs. (43a,b).

## D. Synopsis of Analog Spectral Equations

Analog frequency-domain equations have been derived stepwise by fourier transformation of the analog space- and time-domain equations. Each transformation gave a product of two spectra, one representing a physical process, the other characterizing the result of all prior processes. Thus functions representing analog output spectra from scanning and staring sensors are obtained by substituting Eqs. (43a,b) and (40a,b) into Eqs. (46a,b) respectively:

$$S_{\lambda f}(f,k_y;T)/R_\lambda = \frac{1}{\zeta}\cdot U_{b\lambda}(f/\zeta,k_y;T)\cdot P_\lambda(f/\zeta,k_y)\cdot\Gamma(f/\zeta,k_y)\cdot H(f)$$

$$= \frac{1}{\zeta}\cdot U_{b\lambda}(k_x,k_y;T)\cdot P_\lambda(k_x,k_y)\cdot\Gamma(k_x,k_y)\cdot H(\zeta k_x) \qquad (47a)$$

$$S_{\lambda f}(k_x,k_y,f)/R_\lambda = U_{b\lambda}(k_x,k_y,f)\cdot P_\lambda(k_x,k_y)\cdot\Gamma(k_x,k_y)\cdot H(f) \qquad (47b)$$

The quantities on the right sides of Eqs. (47a and b) are the apparent object-irradiance spectrum ($U_{b\lambda}$), the monochromatic optical transfer function ($P_\lambda$), the detector transfer function ($\Gamma$), and the overall transfer function (H) for all stages of linear, shift-invariant, analog processing. H includes the effects of any temporal integration during sampling. Eqs. (39a and b) can be used to express $U_{b\lambda}$ in terms of the fourier spectrum $N_{b\lambda}$ of the object radiance. $S_{\lambda f}$ can be regarded as the fourier spectrum of a pseudoimage, i.e., as the spectrum ($U_{b\lambda}\cdot P_\lambda$) of the actual image modified by the detector and analog transfer functions, $\Gamma$ and H. With detector responsivity $R_\lambda$ in [volts/watt], typical units of $S_{\lambda f}$ are [volts/(micron·rcm·hz)] or [volts/(micron·rcm$^2$·hz)] for scanning or staring sensors respectively.

## E. Fourier Spectra of Sampled Pseudoimages

Transforming Eqs. (24a and b) by means of Eqs. (30) and (37) gives

the spectra of instantaneously sampled outputs from scanning and staring sensors:

$$V_{\lambda f}(f,k_y;T) \equiv {}^{2}F[\dot{v}_{\lambda f}(\tau,\beta;T)] \quad [\text{volts}\cdot(\text{micron}\cdot\text{rcm}\cdot\text{hz})^{-1}/(\text{cm}\cdot\text{sec})]$$

$$= {}^{2}F\left[s_{\lambda f}(\tau,\beta;T)\cdot\sum_{l=-\infty}^{\infty}\delta(\tau-l\Delta t)\cdot\sum_{m=-\infty}^{\infty}\delta(\beta-m\Delta y)\right]$$

$$= S_{\lambda f}(f^{o},k_y^{o};T)\bullet\left\{\Delta f\sum_{l=-\infty}^{\infty}\delta[(f-l\Delta f)-f^{o}]\right\}\bullet\left\{\Delta k_y\sum_{m=-\infty}^{\infty}\delta[(k_y-m\Delta k_y)-k_y^{o}]\right\} \quad (48a)$$

$$V_{\lambda f}(k_x,k_y,f) \equiv {}^{3}F[\dot{v}_{\lambda f}(\alpha,\beta,\tau)] \quad [\text{volts}\cdot(\text{micron}\cdot\text{rcm}^{2}\cdot\text{hz})^{-1}/(\text{cm}^{2}\cdot\text{sec})]$$

$$= {}^{3}F\left[s_{\lambda f}(\alpha,\beta,\tau)\cdot\sum_{l=-\infty}^{\infty}\delta(\alpha-l\Delta x)\cdot\sum_{m=-\infty}^{\infty}\delta(\beta-m\Delta y)\cdot\sum_{n=-\infty}^{\infty}\delta(\tau-n\Delta T)\right]$$

$$= S_{\lambda f}(k_x^{o},k_y^{o},f^{o})\bullet\left\{\Delta k_x\sum_{l=-\infty}^{\infty}\delta[(k_x-l\Delta k_x)-k_x^{o}]\right\}$$

$$\bullet\left\{\Delta k_y\sum_{m=-\infty}^{\infty}\delta[(k_y-m\Delta k_y)-k_y^{o}]\right\}\bullet\left\{\Delta F\sum_{n=-\infty}^{\infty}\delta[(f-n\Delta F)]-f^{o}]\right\} \quad (48b)$$

Here $\Delta k_x = (1/\Delta x)$, $\Delta k_y = (1/\Delta y)$, $\Delta f = (1/\Delta t)$, and $\Delta F = (1/\Delta T)$. The replicating property of convolution with a delta function (ref. 3, p. 268; ref. 4, p. 79) can be used to express Eqs. (48a and b) more compactly as follows:

$$V_{\lambda f}(f,k_y;T) = (\Delta f\cdot\Delta k_y)\sum_{l,m=-\infty}^{\infty}\sum S_{\lambda f}[(f-l\Delta f),(k_y-m\Delta k_y);T] \quad (49a)$$

$$V_{\lambda f}(k_x,k_y,f) =$$

$$(\Delta k_x\cdot\Delta k_y\cdot\Delta F)\sum_{l,m,n=-\infty}^{\infty}\sum\sum S_{\lambda f}[(k_x-l\Delta k_x),(k_y-m\Delta k_y),(f-n\Delta F)] \quad (49b)$$

Eqs. (48a,b) and (49a,b) also represent spectra of integrally sampled outputs if $\dot{v}_{\lambda f}$ in Eqs. (48a,b) is replaced by $\langle\dot{v}_{\lambda f}\rangle$ from Eqs. (26a,b).

Eqs. (49a,b) are the results expected by analogy with the familiar 1-D temporal case: The sampled-output spectra $V_{\lambda f}$ consist of replicas of the pseudoimage spectra $S_{\lambda f}$. The replicas are separated by frequency

intervals ($\Delta f = \zeta \Delta k_x, \Delta k_y$) with a scanning sensor and ($\Delta k_x, \Delta k_y, \Delta F$) with a staring sensor. The replicas overlap and aliasing occurs unless the highest frequencies in $S_{\lambda f}$ are less than half the respective frequency intervals. As already explained, spatial integration of the image by the detector acts as a low-pass filter, and temporal integration of the output during sampling does the same. Thus spatial and temporal integration reduce aliasing of the pseudoimage spectra.[24]

## F. Fourier Spectra of Sampled and Cropped Pseudoimages

The spectrum of a single instantaneously sampled and cropped image is obtained by transforming Eq. (28a or b) with Eqs. (30) and (37). The image with epoch T = 0 is specified in the scanning case and selected by the cropping function in the staring case. The results are as follows:

$$\tilde{V}_{\lambda f}(f,k_y;T=0) = {}^2F[\backslash \dot{v}_{\lambda f}(\tau,\beta;T=0)\backslash] \quad [\text{volts}\cdot(\text{micron}\cdot\text{rcm}\cdot\text{hz})^{-1}/(\text{cm}\cdot\text{sec})]$$

$$= {}^2F\left[\dot{v}_{\lambda f}(\tau,\beta;T=0)\cdot \text{rect}\left(\frac{\tau-(L-1)(\Delta t/2)}{L\Delta t}\right)\cdot \text{rect}\left(\frac{\beta-(M-1)(\Delta y/2)}{M\Delta y}\right)\right]$$

$$= V_{\lambda f}(f^o,k_y^o;T=0)$$
$$\cdot\{(L/\Delta f)\cdot \text{sinc}[(f-f^o)(L/\Delta f)]\cdot \exp[-i\pi(f-f^o)(L-1)/\Delta f]\}$$
$$\cdot\{(M/\Delta k_y)\cdot \text{sinc}[(k_y-k_y^o)(M/\Delta k_y)]\cdot \exp[-i\pi(k_y-k_y^o)(M-1)/\Delta k_y]\} \quad (50a)$$

$$\tilde{V}_{\lambda f}(k_x,k_y,f) = {}^3F[\backslash \dot{v}_{\lambda f}(\alpha,\beta,\tau)\backslash] \quad [\text{volts}\cdot(\text{micron}\cdot\text{rcm}^2\cdot\text{hz})^{-1}/(\text{cm}^2\cdot\text{sec})]$$

$$= {}^3F\left[\dot{v}_{\lambda f}(\alpha,\beta,\tau)\cdot \text{rect}\left(\frac{\alpha-(L-1)(\Delta x/2)}{L\Delta x}\right)\cdot \text{rect}\left(\frac{\beta-(M-1)(\Delta y/2)}{M\Delta y}\right)\cdot \text{rect}(\tau/\Delta T)\right]$$

$$= V_{\lambda f}(k_x^o,k_y^o,f^o)$$
$$\cdot\{(L/\Delta k_x)\cdot \text{sinc}[(k_x-k_x^o)(L/\Delta k_x)]\cdot \exp[-i\pi(k_x-k_x^o)(L-1)/\Delta k_x]\}$$
$$\cdot\{(M/\Delta k_y)\cdot \text{sinc}[(k_y-k_y^o)(M/\Delta k_y)]\cdot \exp[-i\pi(k_y-k_y^o)(M-1)/\Delta k_y]\}$$
$$\cdot\{(1/\Delta F)\cdot \text{sinc}[(f-f^o)/\Delta F]\} \quad (50b)$$

The complex exponential phase factors in these equations can be eliminated by centering the rectangle functions on the origin, but then the lower limits of the corresponding spatial and temporal sums are negative instead of zero.

Substituting $V_{\lambda f}(f^o,k_y^o;T=0)$ and $V_{\lambda f}(k_x^o,k_y^o,f^o)$ from Eqs. (49a,b) into Eqs. (50a,b) gives the following more informative expressions for $\tilde{V}_{\lambda f}$:

$$\tilde{V}_{\lambda f}(f,k_y;T=0) = (L\cdot M)\sum_{l,m=-\infty}^{\infty} S_{\lambda f}[(f^\circ-l\Delta f),(k_y^\circ-m\Delta k_y);T=0]$$
$$\cdot\{\mathrm{sinc}[(f-f^\circ)(L/\Delta f)]\cdot\exp[-i\pi(f-f^\circ)(L-1)/\Delta f]\}$$
$$\cdot\{\mathrm{sinc}[(k_y-k_y^\circ)(M/\Delta k_y)]\cdot\exp[-i\pi(k_y-k_y^\circ)(M-1)/\Delta k_y]\} \quad (51a)$$

$$\tilde{V}_{\lambda f}(k_x,k_y,f) = (L\cdot M)\sum_{l,m,n=-\infty}^{\infty} S_{\lambda f}[(k_x^\circ-l\Delta k_x),(k_y^\circ-m\Delta k_y),(f^\circ-n\Delta F)]$$
$$\cdot\{\mathrm{sinc}[(k_x-k_x^\circ)(L/\Delta k_x)]\cdot\exp[-i\pi(k_x-k_x^\circ)(L-1)/\Delta k_x]\}$$
$$\cdot\{\mathrm{sinc}[(k_y-k_y^\circ)(M/\Delta k_y)]\cdot\exp[-i\pi(k_y-k_y^\circ)(M-1)/\Delta k_y]\}$$
$$\cdot\mathrm{sinc}[(f-f^\circ)/\Delta F] \quad (51b)$$

Eqs. (51a and b) state that truncating the sensor output broadens and distorts ("ripples") the pseudoimage spectra $S_{\lambda f}$ by convolving them with the transforms of the cropping functions. The broadening worsens the effects of aliasing in the sampled and cropped output. Recording large images (making L and M large) moves the first zeros of the corresponding sinc functions to lower frequencies and reduces broadening along the associated frequency axes. Recording many images from a starer similarly reduces broadening along the temporal frequency axis since (N/ΔF) replaces (1/ΔF) in Eq. (50b).

Eqs. (50a,b) and (51a,b) also represent spectra of integrally sampled and cropped outputs if $\backslash\dot{v}_{\lambda f}\backslash$ is replaced in Eqs. (50a,b) by $\backslash\langle\dot{v}_{\lambda f}\rangle\backslash$ from Eqs. (29a,b).

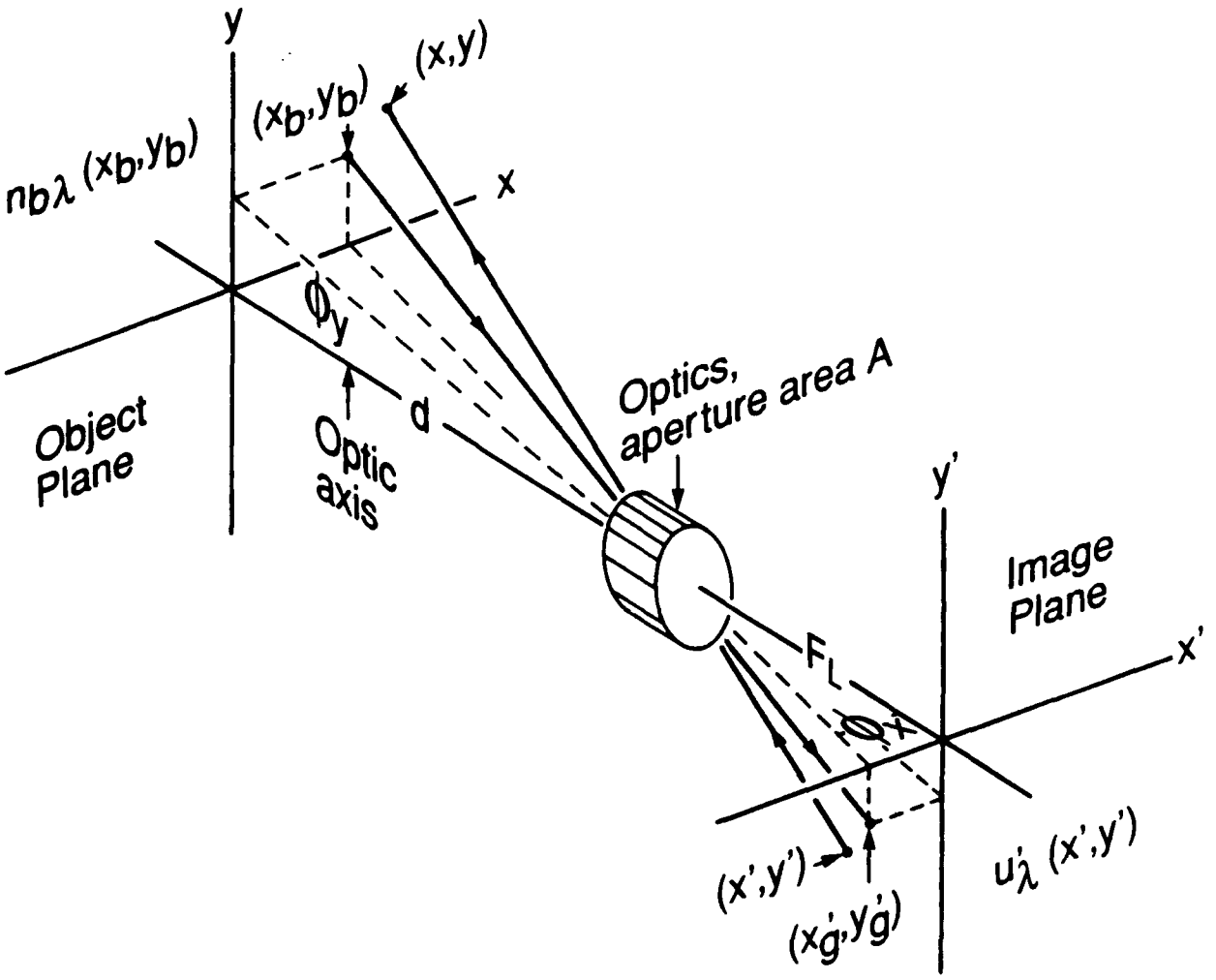


Fig. 1 — Schematic diagram of electro-optic sensor viewing distant scene.

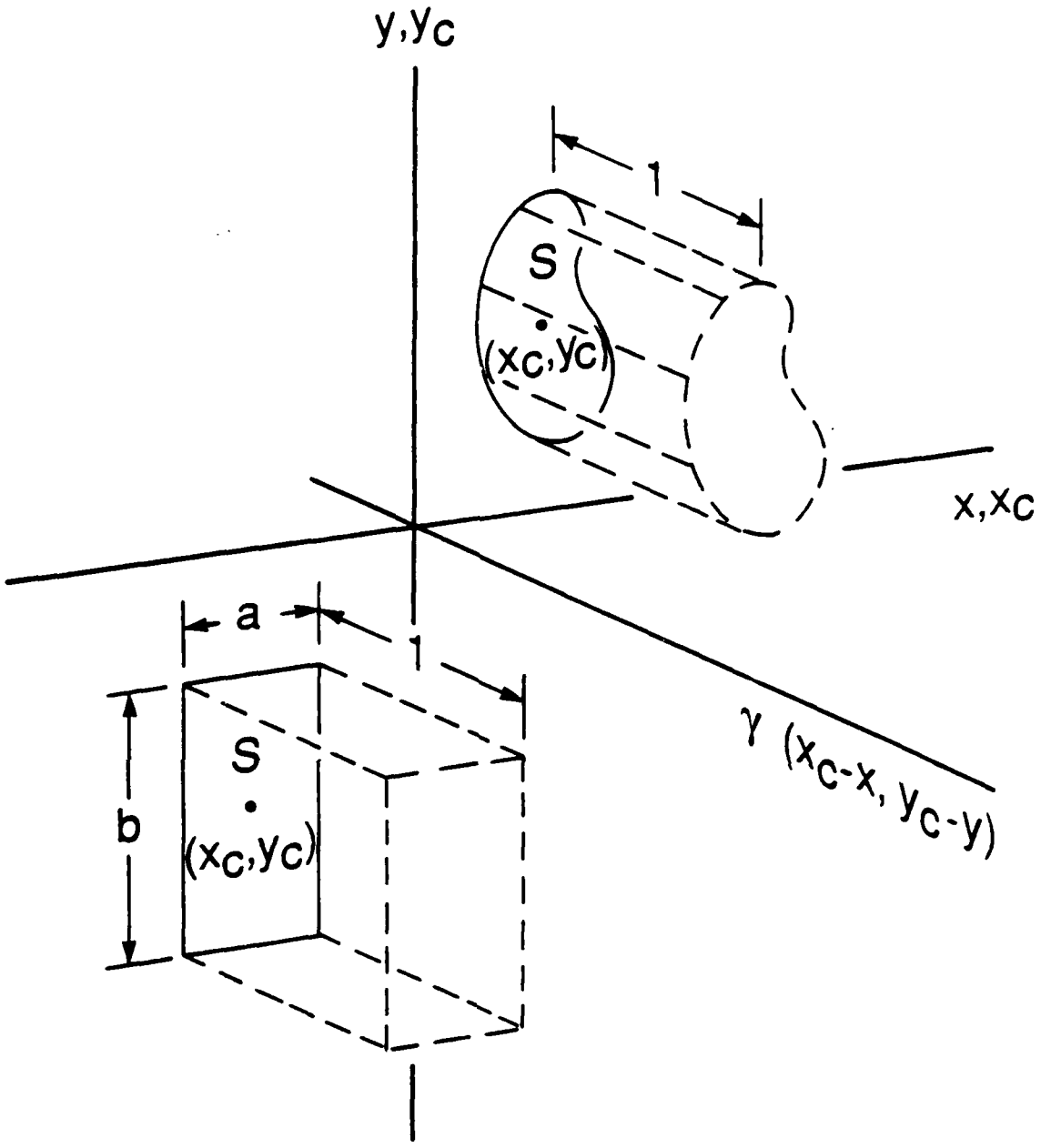


Fig. 2 — Zero-one response functions, Eqs. (16) and (18), for arbitrarily-shaped and rectangular detectors with constant responsivity on their surfaces S. Note distinction between image (x,y) and detector-center ($x_c$,$y_c$) variables.

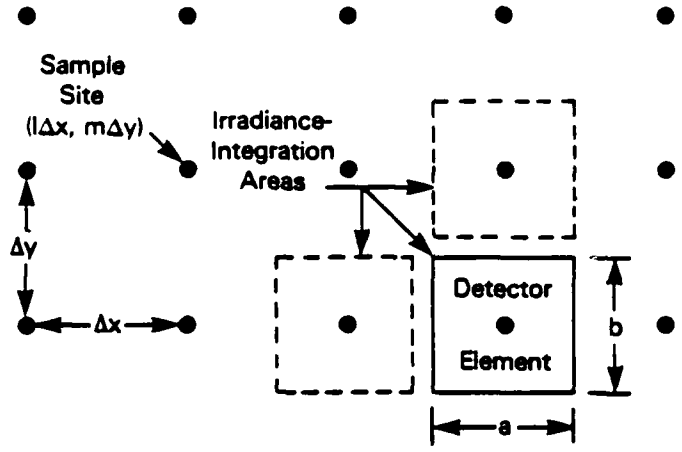


(a) Staring Sensor

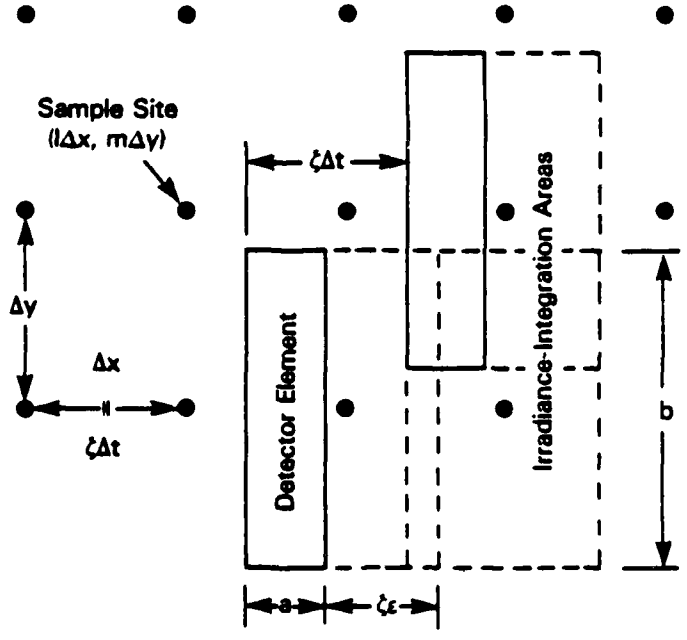


(b) Scanning Sensor

Fig. 3 — Sampling geometries for staring and scanning sensors with channel offsets removed from scanner output.

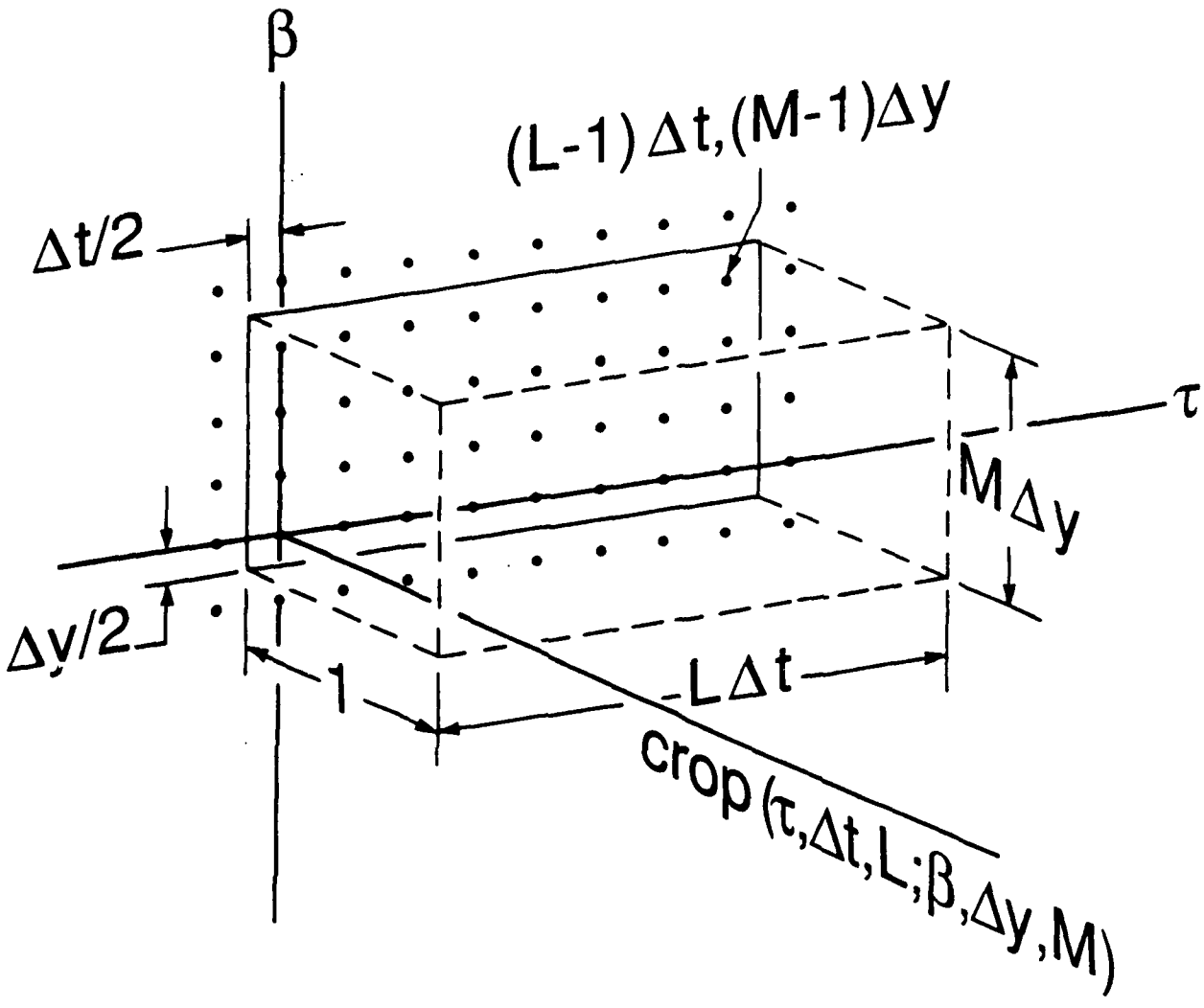


Fig. 4 — Rectangular image-cropping (zero-one) function Eq. (27a) that provides M rows and L columns of samples.

## APPENDIX A. 2-D Fourier Transform of a Convolution, Eq. (36a')

To simplify notation let $\int^2 \equiv \int\int_{-\infty}^{\infty}$ and

$$c(\zeta t, y_c; T) \equiv \int^2 g(x,y;T)\cdot w(\zeta t-x, y_c-y)\cdot dxdy. \tag{A1}$$

Then from Eq. (30)

$${}^2F[c] = \int^2 \left\{\int^2 g(x,y;T)\cdot w(\zeta t-x, y_c-y)\cdot dxdy\right\}\cdot \exp[-i2\pi(ft+k_y y_c)]\cdot dtdy_c. \tag{A2}$$

Change the order of the double integrations.

$${}^2F[c] = \int^2 g(x,y;T)\left\{\int^2 w(\zeta t-x, y_c-y)\cdot \exp[-i2\pi(ft+k_y y_c)]\cdot dtdy_c\right\}\cdot dxdy. \tag{A3}$$

Multiply the outer integrand by $1 = \exp[-i2\pi(k_x x+k_y y)]\cdot\exp[-i2\pi(-k_x x-k_y y)]$.

$${}^2F[c] = \int^2 g(x,y;T)\cdot \exp[-i2\pi(k_x x+k_y y)]\cdot \left\{\int^2 w(\zeta t-x, y_c-y)\cdot \exp[-i2\pi(ft+k_y y_c)]\cdot dtdy_c\right\}\cdot \exp[-i2\pi(-k_x x-k_y y)]\cdot dxdy. \tag{A4}$$

Combine the final exponential with the inner integrand.

$${}^2F[c] = \int^2 g(x,y;T)\cdot \exp[-i2\pi(k_x x+k_y y)]\cdot \left\{\int^2 w(\zeta t-x, y_c-y)\cdot \exp\{-i2\pi[(ft-k_x x)+k_y(y_c-y)]\}\cdot dtdy_c\right\}\cdot dxdy. \tag{A5}$$

Substitute $f=\zeta k_x$, $\zeta t=x_c$, and $dt=dx_c/\zeta$ into the inner double integral.

$${}^2F[c] = \int^2 g(x,y;T)\cdot \exp[-i2\pi(k_x x+k_y y)]\cdot \left\{\frac{1}{\zeta}\cdot\int^2 w(x_c-x, y_c-y)\cdot \exp\{-i2\pi[k_x(x_c-x)+k_y(y_c-y)]\}\cdot dx_c dy_c\right\}\cdot dxdy. \tag{A6}$$

Change the inner variables of integration to $X=(x_c-x)$, $Y=(y_c-y)$, and regroup the terms of the outer double integral.

$$2_{F[c]} = \left\{\int^2 g(x,y;T)\cdot\exp[-i2\pi(k_x x+k_y y)]\cdot dxdy\right\}\cdot$$

$$\left\{\frac{1}{\zeta}\cdot\int^2 w(X,Y)\cdot\exp[-i2\pi(k_x x+k_y y)]\cdot dXdY\right\} \qquad (A7)$$

$$= G(k_x,k_y;T)\cdot\frac{1}{\zeta}\tilde{w}(k_x,k_y) \qquad (36a')$$

## APPENDIX B. 3-D Fourier Transform of a Product, Eq. (37)

To simplify notation let $\int \equiv \int_{-\infty}^{\infty}$, $\int^3 \equiv \iiint_{-\infty}^{\infty}$, and

$$\rho(x,y,t) \equiv g(x,y,t)\cdot q(x)\cdot w(y)\cdot z(t). \tag{B1}$$

Then from Eq. (30)

$${}^3F[\rho] = \int^3 \{g(x,y,t)\cdot q(x)\cdot w(y)\cdot z(t)\}\cdot \exp[-i2\pi(k_x x+k_y y+ft)]\cdot dxdydt. \tag{B2}$$

Replace g(x,y,t) by the inverse transform of its spectrum Eq. (31).

$${}^3F[\rho] = \int^3 \left\{ \int^3 G(k_x^o,k_y^o,f^o)\cdot \exp[i2\pi(k_x^o x+k_y^o y+f^o t)]\cdot dk_x^o dk_y^o df^o \right\}\cdot$$

$$\{q(x)\cdot w(y)\cdot z(t)\}\cdot \exp[-i2\pi(k_x x+k_y y+ft)]\cdot dxdydt \tag{B3}$$

Change the order of the triple integrals and combine the exponentials.

$${}^3F[\rho] = \int^3 \left\{ \int^3 \{q\cdot w\cdot z\}\cdot \exp\{-i2\pi[(k_x-k_x^o)x+(k_y-k_y^o)y+(f-f^o)t]\}\cdot dxdydt \right\}\cdot$$

$$G(k_x^o,k_y^o,f^o)\cdot dk_x^o dk_y^o df^o \tag{B4}$$

Factor the inner triple integral into its separable parts.

$${}^3F[\rho] = \int^3 \left\{ \int q(x)\cdot \exp[-i2\pi(k_x-k_x^o)x]\cdot dx\cdot \right.$$

$$\int w(y)\cdot \exp[-i2\pi(k_y-k_y^o)y]\cdot dy\cdot$$

$$\left. \int z(t)\cdot \exp[-i2\pi(f-f^o)t]\cdot dt \right\}\cdot G(k_x^o,k_y^o,f^o)\cdot dk_x^o dk_y^o df^o \tag{B5}$$

The inner integrals are the fourier spectra of q(x), w(y), and z(t).

$${}^3F[\rho] = \int^3 G(k_x^o,k_y^o,f^o)\cdot [Q(k_x-k_x^o)\cdot W(k_y-k_y^o)\cdot Z(f-f^o)]\cdot dk_x^o dk_y^o df^o \tag{B6}$$

This 3-D convolution can be written symbolically in two ways:

$${}^3F[\rho] = G(k_x^o,k_y^o,f^o) \circledcirc\circledcirc\circledcirc [Q(k_x-k_x^o)\cdot W(k_y-k_y^o)\cdot Z(f-f^o)] \tag{B7}$$

$$= G(k_x^o,k_y^o,f^o) \circledcirc Q(k_x-k_x^o) \circledcirc W(k_y-k_y^o) \circledcirc Z(f-f^o) \tag{37}$$

## APPENDIX C. Equivalence of Projection-Slice and Present Analyses when the Former Applies

Using a projection-slice approach, reference 9 derives relations for the output and its spectrum from a scanning sensor. Here more general relations are derived differently. If both approaches are correct, they should give the same result when both are applicable. This appendix demonstrates the equivalence. The simpler projection-slice approach is preferable for treating output from a single detector or from a two-dimensional spatial filter.[8] The present analysis is better for dealing with images.

For comparison of the two approaches, results of this analysis must be rewritten using the notation and conventions of reference 9. The space, time, and frequency coordinates are the same in the two works, as are the fourier-transform definitions except for the minor notational difference $F_2 = {}^2F$. Use of normalized scale factors in reference 9 corresponds to projecting the image irradiance distribution ideally onto the object plane, as in the present work. The "intensity image distribution function" of reference 9 is the same as the "image irradiance distribution" of this work. Conversions for other quantities are:

$$(o=u_{b\lambda},\ O=U_{b\lambda}) \quad (h_s=p_\lambda,\ H_s=P_\lambda) \quad (i=u_\lambda,\ I=U_\lambda) \quad (d=\gamma,\ D=\Gamma)$$

$$(i'=s_\lambda/R_\lambda,\ I'=S_\lambda/R_\lambda) \quad (R=R_\lambda,\ b=\zeta,\ \omega=2\pi f)$$

$$[v(t)=s_{\lambda f}(\tau;\beta=0),\ H(\omega)=S_{\lambda f}(f;\beta=0)]$$

The two conversions in brackets apply when there is no analog processing - i.e., $[h(\tau-t)=\delta(\tau-t),\ H(f)=1]$ - and voltage units are used for detector responsivity. Further differences between the notation of reference 9 and this work are as follows: Here P is the optical transfer function, in reference 9 it is the projection of I' on y=0. A prime denotes any image-plane quantity in this work, in reference 9 it indicates image irradiance convolved with the detector function d=γ. Finally, reference 9 does not distinguish between different temporal quantities such as (t,τ,T) or different spatial quantities such as (x,y), $(x_c,y_c)$, (α,β).

The key results of reference 9 are now derived from the results of the present work. From Eqs. (20a), (31), and (46a)

$$s_{\lambda f}(\tau,\beta) = {}^{-2}F[S_{\lambda f}(f,k_y)]$$

$$= \int_{-\infty}^{\infty}\int \frac{1}{\zeta} S_\lambda(f/\zeta,k_y)\cdot H(f)\cdot \exp[i2\pi(f\tau+k_y\beta)]\cdot df dk_y. \qquad (C1)$$

Substitution of $f=\zeta k_x$ and $H(f)=H(\zeta k_x)$, some rearrangement, and definition of a new quantity give

$$s_{\lambda f}(\tau,\beta) = \int_{-\infty}^{\infty} H(\zeta k_x)\cdot Pr(k_x,\beta)\cdot\exp(i2\pi k_x\zeta\tau)\cdot dk_x, \qquad (C2)$$

where $Pr(k_x,\beta)$ is the projection of $S_\lambda$ on $y=\beta$:

$$Pr(k_x,\beta) = \int_{-\infty}^{\infty} S_\lambda(k_x,k_y)\cdot\exp(i2\pi k_y\beta)\cdot dk_y. \qquad (C3)$$

It follows from the definitions of independent coordinates, functions, and equality that

$$s_{\lambda f}(\tau;\beta=0) = \int_{-\infty}^{\infty} H(\zeta k_x)\cdot Pr(k_x;\beta=0)\cdot\exp(i2\pi k_x\zeta\tau)\cdot dk_x. \qquad (C4)$$

(Since all coordinates are independent, any can be fixed at an arbitrary value without regard to the others, and the value must be the same on the two sides of the functional equality.) When, as in reference 9, there is no analog processing, $H(\zeta k_x) = H(f) = 1$ and

$$s_{\lambda f}(\tau;\beta=0) = \int_{-\infty}^{\infty} Pr(k_x;\beta=0)\cdot\exp(i2\pi k_x\zeta\tau)\cdot dk_x. \qquad (C5)$$

With the appropriate conversions this becomes Eq. (9) of reference 9:

$$v(t) = R\cdot\int_{-\infty}^{\infty} P(k_x)\cdot\exp(i2\pi k_x bt)\cdot dk_x = R\cdot i'(bt,0) \qquad \text{Ref. 9, Eq. (9)}$$

Fourier transforming Eq. (C5) using Eq. (30) gives

$$S_{\lambda f}(f;\beta=0) = {}^1F[s_{\lambda f}(\tau;\beta=0)]$$

$$= \int_{-\infty}^{\infty}\left[\int_{-\infty}^{\infty} Pr(k_x;\beta=0)\cdot\exp(i2\pi k_x\zeta\tau)\cdot dk_x\right]\cdot\exp(-i2\pi f\tau)\cdot d\tau. \qquad (C6)$$

After substituting $f=\zeta k_x$, $\sigma=\zeta\tau$, and recalling that $(\alpha,k_x)$ are conjugate

variables, one obtains

$$S_{\lambda f}(f;\beta=0) = \frac{1}{\zeta}\cdot\int_{-\infty}^{\infty}\left[\int_{-\infty}^{\infty} Pr(k_x;\beta=0)\cdot\exp(i2\pi k_x\alpha)\cdot dk_x\right]\cdot\exp(-i2\pi k_x\alpha)\cdot d\alpha$$

$$= \frac{1}{\zeta}\cdot 1_F\{^{-1}_F[Pr(k_x;\beta=0)]\} = \frac{1}{\zeta}\cdot Pr(k_x;\beta=0). \qquad (C7)$$

On conversion of notation the last equality becomes

$$H(\omega) = \frac{R}{b}\cdot P(k_x) = \frac{R}{b}\cdot P(\omega/2\pi b). \qquad (C8)$$

This agrees with Eq. (10) of reference 9 when typographical errors in that equation are corrected by derivation as follows.

$$H(\omega) = \int_{-\infty}^{\infty} v(t)\cdot\exp(-i\omega t)\cdot dt = \frac{R}{b}\cdot\int_{-\infty}^{\infty} i'(x,0)\cdot\exp(-i2\pi k_x x)\cdot dx$$

$$= \frac{R}{b}\int_{-\infty}^{\infty}\left[\int_{-\infty}^{\infty} P(k_x)\cdot\exp(i2\pi k_x x)\cdot dx\right]\cdot\exp(-i2\pi k_x x)\cdot dx = \frac{R}{b}\cdot F_1\{\bar{F}_1^{1}[P(k_x)]\}$$

$$= \frac{R}{b}\cdot P(k_x) = \frac{R}{b}\cdot P(\omega/2\pi b) \qquad \text{Ref. 9, Eq. (10)}$$

## REFERENCES


1. E. B. Brown, Modern Optics (Reinhold, New York, 1965).
2. C. L. Wyatt, Radiometric Calibration: Theory and Methods (Academic Press, New York, 1978).
3. J. D. Gaskill, Linear Systems, Fourier Transforms, and Optics (Wiley, New York, 1978).
4. R. N. Bracewell, The Fourier Transform and Its Applications (McGraw-Hill, New York, 1978), 2nd ed..
5. P. B. Fellgett and E. H. Linfoot, "On the assessment of optical images," Phil. Trans. Roy. Soc. 247, 369 (1955).
6. E. H. Linfoot, Fourier Methods in Optical Image Evaluation (Focal Press, London, 1964).
7. W. K. Pratt, Digital Image Processing (Wiley, New York, 1978).
8. W. N. Peters, "One- and two-dimensional matched filter for scanning electro-optic systems," J. Opt. Soc. Am. A3, 347 (1986).
9. W. N. Peters and D. A. Scribner, "Transformation for the unified linear analysis of optics and electronics," Appl. Opt. 24, 1247 (1985).
10. N. S. Kopeika, S. Solomon, and Y. Gencay, "Wavelength variation of visible and near-infrared resolution through the atmosphere: dependence on aerosol and meteorological conditions," J. Opt. Soc. Am. 71, 892 (1981).
11. A. Ishimaru, "Limitation on image resolution imposed by a random medium," Appl. Opt. 17, 348 (1978).
12. K. T. Knox and B. J. Thompson, "Recovery of images from atmospherically degraded short-exposure photographs," Astrophys. J. 193, L45 (1974).
13. W. Swindell, "A noncoherent optical analog image processor," Appl. Opt. 9, 2459 (1970).
14. D. Korff, G. Dryden, and R. P. Leavitt, "Isoplanicity: The translation invariance of the atmospheric Green's function," J. Opt. Soc. Am. 65, 1321 (1975).
15. J. W. Goodman, Introduction to Fourier Optics (McGraw-Hill, New York, 1968).
16. A. D. Schnitzler, "Analysis of Noise-Required Contrast and Modulation in Image-Detecting and Display Systems," in Perception of Displayed Information (Plenum Press, New York, 1973), edited by L. M. Biberman.
17. A. Papoulis, Systems and Transforms with Applications in Optics (Robert E. Krieger Publishing Co., Malabar, FL, 1981).
18. J. A. Jamieson et al., Infrared Physics and Engineering (McGraw-Hill, New York, 1963).
19. E. L. O'Neill, "Transfer function for an annular aperture," J. Opt. Soc. Am. 46, 285 (1956).

20. G. F. Aroyan, "The technique of spatial filtering," Proc. IRE 47, 1561 (1959).
21. R. H. Grube, "A method for obtaining the transfer functions of space filters by differential superpositions," Infrared Phys. 2, 61 (1962).
22. S. Tutumi, "Spatial filter used in Scanning optical detection system," Electronics and Communications in Japan 49, no. 6, 13 (1966).
23. W. Gough and R. P. Williams, "On the notation of the convolution integral," Optica Acta 21, 923 (1973).
24. W. Schneider and W. Fink, "Integral sampling in optics," Optica Acta 23, 1011 (1976).
25. R. Legault, "The Aliasing Problems in Two-Dimensional Sampled Imagery," in Perception of Displayed Information (Plenum Press, New York, 1973), edited by L. M. Biberman.
26. L. J. Pinson. Electro-optics (Wiley, New York, 1986).
27. J. M. Lloyd, Thermal Imaging Systems (Plenum Press, New York, 1975).
28. E. O. Brigham, The Fast Fourier Transform (Prentice-Hall, Englewood Cliffs, NJ, 1974).
29. B. C. Kuo, Digital Control Systems (Holt, Rinehart and Winston, New York, 1980).
30. E. I. Jury, Sampled-Data Control Systems (Wiley, New York, 1958).
31. J. T. Tou, Digital and Sampled-Data Control Systems (McGraw-Hill, New York, 1959).
32. G. Farmanfarma, "General analysis and stability study of finite pulsed feedback systems," AIEE Trans. 77, Pt. II, 148 (1958).
33. G. J. Murphy and H.B. Kennedy, "Closed-loop analysis of sampled-data systems with appreciable pulse width," AIEE Trans. 77, Pt. II, 659 (1959).
34. G. J. Murphy, "On the exact analysis of sampled-data feedback systems with appreciable pulse width," Proc. Nat. Electronics Conf. 17, 214 (1961).
35. C. Y. Lee, "Stability of nonlinear sampled-data systems with finite sampling duration," Proc. IEEE 52, 734 (1964).
36. A. G. J. Holt et al., "Integral sampling," Proc. IEEE 61, 679 (1973).
37. J. J. Hill et al., "Integral sampling networks," Proc. IEEE 62, 1288 (1974).
38. R. D. Stuart, An Introduction to Fourier Analysis (Chapman & Hall and Methuen, London, 1966).
39. K. R. Barnes, The Optical Transfer Function (American Elsevier, New York, 1971).

END

FEB.

1988

DTIC